

1 **A multi-century meteo-hydrological analysis for the Adda river basin (Central**
2 **Alps). Part II: daily runoff (1845–2016) at different scales**

3 R. Ranzi¹, E. M. Michailidi¹, M. Tomirotti¹, A. Crespi^{2,*}, M. Brunetti³ and M. Maugeri^{2,3}

4 ¹ *DICATAM, Università degli Studi di Brescia, Brescia, 25123, Italy*

5 ² *Department of Environmental Science and Policy, Università degli Studi di Milano, Milan,*
6 *20133, Italy.*

7 ³ *Institute of Atmospheric Sciences and Climate, ISAC-CNR, Bologna, 40129, Italy.*

8 ** Now at the Institute for Earth Observation, Eurac Research, Bolzano, 39100, Italy*

9 **Corresponding author:** Alice Crespi, email: alice.crespi@eurac.edu, phone: +39
10 3477777563

11 **Running head:** A multi-century daily runoff record for Adda basin

12 **Keywords:** Long-term trend, daily runoff, Adda basin, evapotranspiration, climate change.

13 **Funding statement:** This research received no specific grant from any funding agency in
14 the public, commercial or not-for-profit sectors

15 **Abstract**

16 A high-quality daily runoff time series of the Lake Como inflow and outflow, the longest for
17 Italian Alps, was reconstructed for the 1845–2016 period in the Adda river basin. It was
18 compared with contemporary monthly precipitation and temperature observations and
19 estimated potential evapotranspiration losses. Trend analyses were conducted for daily flow
20 maxima and 7-day duration minima of inflows into the lake showing a non-significant
21 decrease and a significant increase, respectively. Although the annual precipitation time
22 series exhibits a non-significant decrease, annual runoff volumes decrease with a rate of -136
23 mm century⁻¹, with a significance level of 5%. Possible causes of variability of rainfall and
24 runoff as NAO, AMO and WeMOi indexes and sunspot activity were also explored. Wavelet
25 spectra analyses of monthly precipitation and runoff show some changes in the energy both
26 at small and large scales and are effective in pointing out phenomena as droughts and the
27 effects of dams' regulation. On the other hand, wavelet coherence spectra indicate a weak
28 correlation of NAO and sunspots with precipitation. In addition, the analysis of temperature
29 and potential evapotranspiration tendencies suggests that the decrease of runoff has to be

30 ascribed mostly to anthropogenic factors, including water abstraction for irrigation and
31 increased evapotranspiration losses due to natural afforestation and, only in part, to climatic
32 variability.

33 **1 Introduction**

34 The scientific debate between researchers supporting the concept of the *ever changing*
35 climate characters (Milly et al., 2008) or a pragmatic approach, assuming a stationary random
36 component to explain the variability of hydrological data (Montanari and Koutsoyiannis,
37 2014), relies on the analysis of extended time series of variables but, also, under a clear
38 picture of anthropogenic factors, which may have contributed to the variability of natural
39 systems, such as watersheds. Climate change is a central topic in the agenda of scientists,
40 politicians and the media because, for the first time in almost five billion years of the Earth's
41 history, significant geophysical changes are also occurring due to anthropogenic causes.
42 Humans, according to the large majority of Earth scientists, are inducing an acceleration of
43 changes in the gas composition of the atmosphere and in some components such as the
44 hydrosphere and the cryosphere, to levels which, perhaps, have passed the point of no return
45 (IPCC, 2013; 2014).

46 The community of climatologists and meteorologists has been dedicated for decades in
47 collecting, sharing and processing meteorological data on multi-secular horizons in large
48 transnational geographical areas (e.g. Auer et al., 2007, Brunetti et al., 2009). The
49 geographical fragmentation of river basins in various administrative areas often transnational
50 or transregional, and the difficulties encountered in coordinating the hydrographic services
51 responsible for this task have probably limited the creation of multi-century data sets of daily
52 runoff series. For example, at the Global Runoff Data Center
53 (https://www.bafg.de/GRDC/EN/Home/homepage_node.html) daily runoff data starting
54 before 1850, at the end of the Little Ice Age, are available for only three gauging stations.

55 Multi-decadal analyses of variability and trends of runoff are available at regional and global
56 scale. For instance, a regionally coherent picture of annual streamflow trends in Europe
57 emerged, with negative trends in southern and eastern regions, and generally positive trends
58 elsewhere, from the study of Stahl et al. (2010) for the 1962–2004 period, with fewer stations
59 starting after 1932. Su et al. (2018) recently published the results of the trend analysis for the

60 period 1948–2004 of the monthly and annual outflows of 916 rivers worldwide, flowing into
61 the oceans, showing that for 120 of them the trends are positive, while for 51 they are negative
62 with a statistical significance of 5%. Considering extremes, an important study on a European
63 scale has made it possible to identify variations in the last fifty years, not so much in the
64 intensity of the floods, as in their seasonal distribution (Blöschl et al., 2017).

65 For the Italian basins, Zanchettin et al. (2008a, 2008b) have reconstructed a series of daily
66 runoff for the Po river at Pontelagoscuro, dating back to the beginning of the nineteenth
67 century. Beside a negative trend, they report a highly significant signal in the Fourier
68 spectrum of their deseasonalized monthly runoff record at scale of 12.9 years and they
69 connect it to the solar activity. A number of other authors have searched for such a signature.
70 The first, to the authors' knowledge, to question a possible linkage between sunspot numbers
71 and hydrologic time series were Rodriguez-Iturbe and Yevjevich (1968) who conducted
72 cross-correlation and Fourier spectra analysis and concluded that no significant correlation
73 exists between rainfall or runoff and sunspots. Nevertheless, a wide number of studies
74 examined the effect of sun forcing on variables like discharge, precipitation, sea level and
75 various atmospheric indices (Grinsted et al., 2004; Jevrejeva et al., 2006; Moore et al., 2006;
76 Zanchettin et al., 2008b, 2009) making especially use of wavelet analysis, as an alternative
77 to Fourier transform.

78 Even though many authors have searched for a solar signature in meteorological and
79 hydrological variables in many areas of the world, a clear consensus, based not only on
80 statistical significance but also on strong physical reasoning, cannot be established.
81 Moreover, correlations can be proven to be spurious when they are not accompanied by the
82 appropriate significance levels or when there is a misuse of the available tools. In fact, Moore
83 et al. (2006) have strongly criticized spectrum results with no significance testing or tested
84 only against white-noise, when in reality the investigated climate index time series are lag-1
85 correlated autoregressive processes, and they suggest other plausible mechanisms, as the
86 doubling of the 5.2–5.7 year cycle of the Atlantic Oscillation. Additionally, the use of a cross
87 wavelet spectrum when investigating for cause-effect relations can lead to spurious cross-
88 correlations; one should therefore opt for the wavelet coherence spectrum instead.

89 Apart from searching for the solar signature, wavelet transforms provide a powerful tool
90 offering information in a multi-scale basis, ideal in cases of hydrological and geophysical
91 time series that often exhibit transience. They have therefore been utilized extensively in
92 hydrometeorological contexts focusing both on discharge and lake water level time series
93 (e.g. Smith et al., 1998, Coulabily and Burn, 2004; Labat et al., 2005; Küçük et al., 2009;
94 Rossi et al., 2009; Zolezzi et al., 2009; Carey et al., 2013; Zhang et al., 2014) and on rainfall
95 data (Kumar and Foufoula-Georgiou, 1993; Marazzi et al., 1996; Nakken, 1998; Markovic
96 and Koch, 2005; Labat et al., 2000). Wavelet analysis is also interesting to highlight the effect
97 on runoff of hydropower operation as shown by Zolezzi et al. (2009), who focused their
98 attention on the interpretation of the wavelet power spectrum of streamflow data explaining
99 hydrological alterations - results of climate change or hydropower operations - in the Adige
100 River. Similarly, Zhang et al. (2014) investigated the changes in periodicity for the East
101 River, in China, where the construction of water reservoirs led to a disappearing annual cycle.
102 Other detailed analyses on the variability of the hydrological regime of Po river and some of
103 its sub-basins after 1920 are presented by Montanari (2012) who identified in the daily
104 riverflow time series perturbations whose memory is maintained in the long term and whose
105 long-term persistence increases with the catchment size. Also for the Adige river, in the
106 Central Italian Alps, the analysis of the variability of the daily flow rates was focused on the
107 period after 1923, when official runoff data were published (Zolezzi et al., 2009).
108 Studies dating back to the mid-nineteenth century are however rare and, therefore, a
109 contribution on a new high-quality 172-year long daily runoff series, objective of the present
110 work, is of important scientific value, especially because the analyses are run in parallel with
111 those on the monthly catchment precipitation record, presented in the companion paper by
112 Crespi et al. (this issue).

113 With the objective of investigating and contributing to the knowledge of the variability of
114 surface runoff of Italian rivers on a multi-secular horizon, at the University of Brescia long-
115 term runoff series of rivers in the Italian central Alps, from Adige to Ticino river, are being
116 collected and reconstructed. First results showed a more marked decrease in the annual runoff
117 compared to that of rainfall (Ranzi et al., 2017; 2018a).

118 In this study we present a detailed reconstruction of the Lake Como daily levels at the
119 hydrometer of the Adda river at Fortilizio in Lecco (Figure 1). From the flow measurements
120 and the stage-discharge curve of Fortilizio the daily outflows of Lake Como from 1st January
121 1845 to 31st December 2016 were obtained and, through the continuity equation of the lake,
122 the daily inflows to the lake were also reconstructed. This is the longest time series of daily
123 runoff for Italian Alps. In addition, this series has been compared with monthly precipitation
124 averaged at the catchment scale (Crespi et al., this issue).

125 The objective of the present paper is twofold: i) studying the role of climate change and
126 variability, and natural forcing factors in general, on streamflow over a wide range of time
127 scales; ii) highlighting how human operations altered the hydrological regimes. Specifically,
128 we intend first to compare and cross-validate the tendency of precipitation at the catchment
129 scale and corresponding runoff records over a multi-century monitoring period, as this is an
130 analysis not frequently available in the scientific literature. Then, through wavelet coherence
131 spectra, we are looking for possible links between natural forcings and climatic
132 teleconnections with the observed hydrological patterns. Finally, for those signals which
133 cannot be explained by natural phenomena only, we search for possible anthropic factors
134 influencing the runoff variability.

135 In the following, after a brief description of the Adda river basin and of the data collection
136 and quality check, the criteria for processing the data of the hydrometric lake levels and
137 outflow from the lake outlet at Fortilizio and finally of the daily inflows are described in the
138 second section, where we also present the methods for the statistical analyses of the 172-year
139 series. Results of the analyses are presented in the third section. Finally, in the fourth section,
140 we discuss the results and investigate the possible causes of runoff and runoff coefficient
141 trends.

142 **2 Material and methods**

143 **2.1 Study area**

144 The study area is located in the upper part of the Adda river catchment (Figure 1) in the
145 Central Italian Alps. The Adda river is one of the main left-side tributaries of Po river and
146 drains an area of about 8000 km², 94% of which is in northern Italy and 6% in Switzerland.
147 The upper part of the basin, gauged at the outlet of Lake Como in Lecco, covers an area of

148 4508 km² and is mostly situated over the southern Alpine ridge in the region of Lombardy.
149 This part extends from the sources of Adda river in the Rhaetian Alps and is characterized
150 by a great orographic heterogeneity; its main valley, Valtellina, is oriented from East to West
151 upstream the Lake Como. Being located in a prevalently mountainous environment, this
152 region is characterized by altitude gradients from about 200 m a.s.l. at Lake Como to more
153 than 4050 m a.s.l. at Piz Bernina. Land use is mainly covered by agricultural crops in the
154 valleys, deciduous and coniferous forests, and bare rocks above 2500 m a.s.l..

155 A number of Alpine glaciers, located in the groups of Bernina, Disgrazia and Ortles-
156 Cevedale, are included in this study area, covering today an area of 65 km² (Smiraglia and
157 Diolaiuti, 2015; Salvatore et al., 2015). During the last decades, an intense reduction of
158 glacier coverage and a strong volume loss have been observed (D'Agata et al., 2018). The
159 above loss corresponds to about $5.4 \cdot 10^7$ m³ of water per year, contributing to the basin runoff
160 with a specific depth of 12 mm yr⁻¹. Although this volume appears small (~1%) relative to
161 the total annual precipitation, since it is mainly released during the summer months, it
162 facilitates civil use, agriculture, industry and hydropower production, in periods of high water
163 demand.

164 Due to the elevated water needs, a substantial number of artificial reservoirs has been built
165 between 1920–1969. The lakes of Cancano and S. Giacomo are two of the largest, with a
166 total storage volume of about $188 \cdot 10^6$ m³ of water, mainly used for hydropower generation.
167 The artificial water volume storage complements the volume of the natural water reservoirs,
168 the most important of which is Lake Como with a total surface of 145 km² and a potential
169 storage volume of about $247 \cdot 10^6$ m³, available after the construction of the Olginate barrage,
170 completed in the year 1945. The barrage can control the outflow from the lake in the range
171 of water levels between -0.50 m and + 1.20 m with respect to the null point of the Fortilizio
172 staff gauge. The purpose of the regulation is to manage the water storage for irrigation and
173 hydropower generation downstream and flood control in the lake.

174 **2.2 Data set**

175 **2.2.1 Precipitation**

176 The catchment precipitation time series was reconstructed at monthly resolution as described
177 by Crespi et al. (this issue) for the period 1845–2016. That paper presents also an annual

178 catchment precipitation time series, corrected in order to take into account the systematic
179 underestimation of solid precipitation of rain gauges.

180 **2.2.2 Runoff**

181 Data from two hydrometric stations were used to permit the runoff reconstruction through
182 the use of the continuity equation. The hydrometric station of Fortilizio is located at the lake
183 outlet in Lecco, where a staff gauge was installed over the whole 1845–2016 monitoring
184 period. Part of this time series was collected and quality-checked by accessing to unpublished
185 hydrometric data. Another hydrometric station was installed on the left lake shore at
186 Malpensata (and after 1941 moved to the opposite shore of Lake Como, with the same
187 hydrometric null point), just upstream of the outlet. Additionally, another hydrometric station
188 with regular discharge measurements was installed, after 1940, a few kilometers downstream
189 of the lake in Lavello (Figure 1).

190 For the pre-regulation period (1845–1945), some stage-discharge relationships for the outlet
191 were available from the literature (Figure 2). A first one was proposed by Lombardini (1866),
192 a distinguished hydraulic engineer who studied the runoff regimes of lakes and rivers
193 worldwide, followed by a second one proposed by Fantoli (1921) until 1922 and a third one
194 proposed by Citrini (1977) until 1945, based on energy and mass conservation equations.
195 These curves are very consistent and they are perfectly confirmed by discharge
196 measurements conducted for the same river reach in the period 1923–1943 by the Italian
197 Hydrographic Service and published on the Hydrological Yearbooks (Figure 2). The riverbed
198 material at the lake outlet is composed by boulders, gravels and hard rock and can be
199 considered stable, thus indicating that the stage-discharge curves by Fantoli can be applied
200 to transform the daily water level record into a daily outflow record from the lake for the
201 period prior to 1922. The daily inflows were, then, obtained by solving the continuity
202 equation and using the measured daily outflows and the water level at Malpensata/Malgrate
203 hydrometric stations (Consorzio dell’Adda, 1958). For a short period between September
204 1944 and December 1945, when the preliminary dam operation started and the stage-
205 discharge curves at Fortilizio in Lecco were not reliable to assess the regulated outflow, the
206 runoff measurements at the Fuentes hydrometric station (station nr. 2 in Figure 1) were used

207 to estimate the inflow and the lake continuity equation to assess the outflow. Further details
208 on this issue can be found in Ranzi et al. (2018b).

209 For the post-regulation period (1946–2016) the stage-discharge relationship is substantially
210 changed, as the flow capacity at the outlet increased after the outlet was widened allowing
211 for greater outflows for the same water level (Figure 2).

212 The Lake Como daily water level series for the period 1845–2016 is shown in Figure 3,
213 together with Lake Como inflow and outflow series.

214 For the analysis of the inflow series at Lake Como we present in section 3, two distinctive
215 periods will be considered: from 1845 to 1919, before the construction of the major reservoirs
216 in the upper Adda catchment started, and from 1967 to 2016 when all major reservoirs were
217 completed. For the analysis of the outflow runoff series, the pre-regulation period which
218 started in 1845 and ended in December 1945 will be separated from the post-regulation
219 period starting from January 1946 when the Olginate barrage situated downstream of the city
220 of Lecco (Figure 1) initiated to be operated.

221 **2.2.3 Sunspots, NAO and other indexes**

222 As Zanchettin et al. (2008a, 2008b) report a highly significant solar signature in the Po river
223 runoff record, we considered in our analyses solar activity expressed as sunspot numbers.

224 Monthly averages of sunspot numbers date back to 1749 and are available at
225 <http://solarscience.msfc.nasa.gov/SunspotCycle.shtml>. For this study, only values for the
226 period 1845–2016 were considered and when referring to yearly values were derived by
227 averaging the monthly values within a year.

228 Besides sunspots, some indexes were also used to analyze the link of yearly
229 runoff/precipitation with large scale atmospheric circulation variability.

230 Among them, we considered the North Atlantic Oscillation (NAO) index. NAO is a major
231 climatic teleconnection that influences the European climate, particularly during winter
232 (Osborn, 2011). The index expresses the amplitude of the pressure gradient over the North
233 Atlantic Ocean, which is defined as normalized pressure difference between two extreme
234 stations, located in Iceland and Azores or Gibraltar. Specifically, we used the NAO index
235 monthly record dating back to 1823 developed by Jones et al. (1997), which is regularly
236 updated and freely available at <https://crudata.uea.ac.uk/cru/data/nao/>.

237 Steirou et al. (2017) have carried out an extensive review regarding the possible correlations
238 between NAO and, among else, precipitation showing the variability of Pearson's correlation
239 coefficient within Europe. In particular, the zero correlation line crosses Central Europe and
240 in the Italian Alps a negative correlation of the above variables is observed. Additionally,
241 Wrzesiński and Paluszkiwicz (2011) detected negative links between NAO and mean flow
242 for the majority of the Alpine area, in agreement with the findings of other studies (López-
243 Moreno et al., 2011; Shorthouse and Arnell, 1999; Zanchettin et al., 2008). These results are
244 confirmed by the Adda basin precipitation records which highlight a negative correlation
245 between the two variables at the monthly scale (significant at 5% level for all months,
246 excluding June and September), with correlation coefficient, ρ , ranging from -0.317 to -
247 0.138, and a significant negative correlation for the winter months (December to March),
248 with $\rho=-0.204$ (Figure S1 of the supplementary material).

249 We also considered the Western Mediterranean Oscillation index (WeMOi), defined by
250 means of Padua (45°24'N-11°52'E) and San Fernando (Cádiz) (36°28'N-6°12'W) monthly
251 sea-level pressure values (Martin-Vide and Lopez-Bustins, 2016, data available at:
252 <http://www.ub.edu/gc/en/wemo/>). Also this index highlights significant correlation with the
253 Adda basin precipitation and runoff records. Specifically, significant positive correlations
254 between WeMO index and precipitation were found both at the monthly scale, with ρ values
255 ranging from 0.165 to 0.441, and for the winter months ($\rho=0.379$). Finally, we considered
256 the Atlantic Multidecadal Oscillation (AMO) index, which refers to North Atlantic detrended
257 sea surface temperature. Specifically, we used the record available at NOAA ESRL
258 (<https://www.esrl.noaa.gov/psd/data/timeseries/AMO/>). Some recent papers (see e.g.
259 Zampieri et al., 2017; Brugnara and Maugeri, 2019) seem to indicate a relevant influence of
260 this index on alpine precipitation. However, in our data we found a significant positive
261 correlation of AMO with precipitation only for the month of July ($\rho=0.155$).

262 **2.3 Methods**

263 In order to detect possible trends and their significance in the runoff data, the non-parametric
264 Mann-Kendall (MK) test was employed (Sneyers, 1992), accompanied with Theil-Sen slope
265 estimator (Sen, 1968). The runoff data were also subjected to a running trend analysis,
266 allowing to investigate the trend of each sub-interval of at least 21 years.

267 Besides performing trend analysis, we attempted to decode the signal of the Lake Como
268 inflow and outflow time series of the Adda river, detecting possible changes and variations
269 at different time scales, linked to physical processes or to human interaction. These linkages
270 were sought mainly within processes that have a potentially logical and physically explained
271 cause-effect relationship, namely between the solar forcing, climate indexes and
272 precipitation/runoff. Moreover, a possible influence of the regulation of the reservoirs was
273 considered. Specifically, we applied wavelet analysis to the Adda river catchment runoff and
274 precipitation records and we considered the wavelet coherence-spectra between them and the
275 records of solar sunspots and climate indexes. A practical insight on wavelet theory can be
276 found, among else, in Torrence and Compo (1998) and is briefly presented in the
277 supplementary material. Moreover, we investigated the Lake Como outflow record inspected
278 with the wavelet analysis to point out changes resulting from the lake regulation.

279 **3 Results**

280 **3.1 Climatology of Lake Como inflows and outflows**

281 The average Lake Como inflow in the period 1845–2016 was $165.3 \text{ m}^3 \text{ s}^{-1}$, corresponding to
282 1157 mm yr^{-1} , with maximum mean daily inflow of $2535 \text{ m}^3 \text{ s}^{-1}$, corresponding to 48.6 mm
283 of daily precipitation over the entire investigated catchment, in the most severe flood ever
284 observed which occurred on 3 October 1868. Concerning low flow indexes the minimum
285 inflow with duration of seven days was $11.8 \text{ m}^3 \text{ s}^{-1}$, observed in the year 1922. The month
286 with the highest inflow of 378 mm was October 1993 whereas the year with the highest
287 inflow of 1822 mm was 1872. Comprehensive statistics of inflow and outflow data can be
288 found in Ranzi et al. (2018b).

289 The Lake Como inflow record has a marked seasonality. Focusing on the medians of the
290 values recorded for each day of the year in the 1845–2016 period, the highest values occur
291 at end of May – beginning of June. Then the values decrease in summer and in the first part
292 of autumn, remain almost constant from mid-October to mid-November, decrease again until
293 January, remain almost constant until mid-March and finally increase until the end spring
294 maximum (Figure 4). Moving from the median to higher percentiles, also a second maximum
295 in autumn becomes progressively evident and the highest values generally occur in this
296 season (Figure 4), because it has the strongest skewness of the distributions of the daily

297 inflow values. This strong skewness is also evident from the much higher mean values of the
298 daily inflows with respect to the corresponding median values (Figure 4).

299 In order to investigate the long-term evolution of the yearly cycle of Como Lake inflows and
300 outflows, we considered the records of monthly precipitation, inflow and outflow together
301 with the relative contributions of each month to the corresponding yearly mean values. We
302 compared the yearly cycle of these relative contributions in the period 1845–1919 with the
303 corresponding yearly cycle in the period 1967–2016 to better highlight the effect of reservoirs
304 in the second period, as described in section 2.2.2. This comparison is shown in Figure 5. It
305 highlights a decrease of precipitation in October and an almost unchanged distribution of
306 monthly precipitation throughout the year, when considering the two periods, but also a
307 marked decrease of the seasonality of the Lake Como inflows moving from the first to the
308 second sub-period (Figure 5b). This marked decrease of seasonality, which is not present in
309 the catchment precipitation record (Figure 5a), is due to the reservoirs used for hydropower
310 generation plants, requiring the storage of relevant water volumes during summer and autumn
311 and its release in the cold months of January-April and November-December when the value
312 of energy is higher. Specifically, from June to October 10% of the mean annual runoff was
313 stored in the post-reservoir construction period (1967–2016) in excess to the natural
314 condition period (1845–1919). We recall also that after 1963 a volume corresponding to 20
315 mm of runoff was diverted to the Adda river in the first months of the year from the Spoel
316 watershed, a tributary of the Inn river flowing North of the Alpine ridge.

317 Focusing on Lake Como outflows the most relevant change in the seasonality occurs when
318 the barrage situated just downstream of the city of Lecco began to operate in 1946. By
319 comparing panels b and c in Figure 5, it can be observed that during the lake regulation period
320 the outflow in the months of July and August increases to meet the irrigation demand in the
321 downstream agricultural areas. Runoff increases also in November and December to meet
322 the hydropower generation demand in the downstream reach of the Adda river. The
323 corresponding volumes are stored in the Lake Como mainly during the months of April and
324 May as a result of spring precipitation and snowmelt.

325 **3.2 Long-term trends of annual runoff**

326 The yearly average runoff series at Lake Como gives evidence of a marked decrease in the
327 1845–2016 period (Figure 6 and Table 1). The trend of annual inflow, which is basically the
328 same of outflow as the lake storage is compensated over the years, is significant at the 5%
329 level. Its Theil-Sen slope turns out to be $-136 \text{ mm century}^{-1}$, corresponding to a reduction of
330 $11.8 \pm 3.2\% \text{ century}^{-1}$, which causes a runoff decrease of $233 \pm 63 \text{ mm}$ over the entire
331 investigated period considering standard error estimates. As discussed more in detail by
332 Crespi et al. (this issue), also the yearly record of average catchment precipitation has
333 negative slope. The catchment precipitation decrease is however much lower (see Figure 6)
334 and it is not statistically significant. Therefore, the investigated catchment highlights a strong
335 decrease in the runoff coefficient series ($-6.4 \pm 1.0\% \text{ century}^{-1}$) (Table 1).

336 This decrease can potentially be explained as an effect of the increased evapotranspiration
337 losses, caused by the increase in temperature and by the expansion of the forested areas, as
338 noted for the adjacent Adige basin (Ranzi et al., 2017). Other possible reasons could be the
339 withdrawal of water for irrigation and anti-frost purposes of almost 2200 hectares, cultivated
340 primarily with fruit, vines and corn, upstream of Lake Como, as well as for drinking water
341 purposes (mounting to about $1 \text{ m}^3/\text{s}$ in the last decades).

342 In order to better investigate the temporal trends, a running-trend analysis was performed on
343 the 1845–2016 annual discharge seasonal record. The Theil-Sen slopes and Mann-Kendall
344 significances were computed on windows of increasing width from 20 years up to the entire
345 period spanned by the series and running from the beginning to the end of the record. The
346 results (Figure 7) highlight that all the windows longer than 150 years have 5%-significant
347 negative trend. Moving to shorter periods, the fraction of time windows with high-
348 significance trend becomes lower. However, almost all significant trends are the negative
349 ones, with some of them very relevant, up to $-100 \text{ mm decade}^{-1}$ for periods ending with the
350 severe droughts of the 1940s and the early 2000s. The strongest negative trends concern
351 windows starting in the 1910s and 1920s. They are due to a relative maximum in the runoff
352 yearly record in the first part of the 20th century, followed by a strong runoff reduction in the

353 1940s. It is worth noticing that also some of the windows of the most recent years have
354 negative runoff trends. They are due to the first decade of the 21st century that was very dry.
355 The pattern of the runoff running trends is reflected by a similar pattern of the precipitation
356 running trends observed in Figure 9 of Crespi et al. (this issue). It is worth noticing that also
357 the runoff coefficient follows this pattern, as shown in Figure 10 of Crespi et al. (this issue),
358 as a result of the non-linearity of the runoff response to precipitation forcing, since the
359 transformation of precipitation into runoff is more efficient when precipitation increases.

360 **3.3 Long-term trends of inflow maxima and minima**

361 Also the record of the annual maxima of the daily mean inflow values has negative slope in
362 the period 1845–2016, with a decrease of $-110 \pm 56 \text{ m}^3\text{s}^{-1}\text{century}^{-1}$ (Table 2; Figure 8).
363 However, this trend is not significant at the 5% level.

364 The long-term trend in the annual maxima of daily flow is also evident comparing the annual
365 cycle for the sub-periods 1845–1919 and 1967–2016 (Figure 9). In fact, the comparison
366 between these two periods gives evidence of the decrease of peaks in the second period where
367 no daily maxima exceed $2000 \text{ m}^3\text{s}^{-1}$, while four days with such high floods did occur in the
368 first period. In addition, less skewed statistics of inflow for each day of the year are observed.
369 The decrease of annual maxima is due both to the general decrease of runoff and to the
370 attenuation effect of the alpine reservoirs upstream of the lake, even though the latter effect
371 seems to be much more important than the former one (Malusardi and Moisello, 2003).

372 This anthropic effect is more evident on low flows than on high flows, since, due to the
373 upstream regulation operated by dams, water is stored during periods of abundance and
374 released during periods of high demand or water scarcity. In fact, the annual minima of mean
375 daily runoff of 7 days – index of the low flow regime – has a significantly increasing trend
376 of $16 \pm 1.5 \text{ m}^3 \text{ s}^{-1} \text{ century}^{-1}$ in the investigated period (Figure 10 and Table 2).

377 **3.4 Precipitation and runoff wavelet spectra**

378 In Figure 11 the Morlet6-wavelet spectrum of the monthly precipitation series deseasonalized
379 by subtracting from each monthly data the monthly mean and dividing by the monthly
380 standard deviation is represented (the corresponding spectrum for the non deseasonalized
381 record is reported in Figure S2 of the supplementary material), thus obtaining a 0-mean, 1-
382 unit standard deviation time series which smooths the effect of the annual cycle. Instead, a

383 12-year scale energy peak appears in the wavelet spectrum thus suggesting a possible link
384 with the solar activity as previously discussed for the Po river by Zanchettin et al. (2008a,
385 2008b) and more generally argued by some authors as Dong et al. (2018), with others, as
386 Tsiropoula (2003), being more skeptical towards the existence of a physical mechanism
387 which might result in meaningful linkages. For the monthly inflow data into the Lake Como
388 a 12-year energy peak is still present, together with the annual periodicity (Figure 12). In this
389 case we normalized the series by subtracting the long-term mean and dividing by the standard
390 deviation and so we did not remove the annual cycle, whereas the spectrum we obtain for
391 both normalized and deseasonalized records of daily inflows is reported in Figure S3 of the
392 supplementary material. It is worth noticing that the wavelet spectrum at annual scale exhibits
393 an evident energy loss around 2005 when a severe drought occurred (see also Figure 6), but
394 not in correspondence of the drought in the 1940s. In order to investigate further the wavelet
395 spectrum of both inflow and outflow from the Lake Como, trendlines of the wavelet power
396 spectrum at different scales were plotted for the two periods, before and after 1946 (Figure
397 13), when the lake regulation started with the Olginate barrage.

398 We can observe that the long-term annual scale trends are declining, a confirmation using
399 the wavelet tool that the annual runoff is decreasing, as discussed previously. More
400 interesting is the increasing trend of the 7-day scale fluctuations of inflow, indicating that the
401 progress of the completion of the reservoirs upstream Lake Como after the 1940s introduced
402 an artificial weekly component in the runoff regime, as already observed by Zolezzi et al.
403 (2009) for the Adige river. Even more remarkable is the sudden increase, after 1946, of the
404 2- to 7-day scale fluctuations in the outflows from the lake, indicating that the Olginate
405 barrage operations significantly changed the outflow regime.

406 **3.5 Wavelet coherence spectra**

407 Because of the observed energy at about 12-year scale, we subjected the Adda river
408 precipitation and runoff time series to a wavelet coherence analysis considering them
409 together to the sunspot and the climate index records.

410 The wavelet coherence between the monthly sunspots and precipitation results in a very
411 unclear picture (Figure 14). As it is seen, no consistent significant wavelet coherence areas
412 are depicted inside the Cone Of Influence (COI). The same results are supported by the

413 wavelet coherence spectrum of sunspots and precipitation after deseasonalization (depicted
414 in Figure S4 of the supplementary material) where only few and scattered areas of significant
415 coherence are present. Also the deseasonalized runoff-sunspots coherence spectra (depicted
416 in Figure S5 of the supplementary material) do not indicate any highly clear coherence and
417 neither the correlation between precipitation and sunspots is significantly different from zero.
418 Therefore, the common energy peak observed around the 11–12 year scale in the
419 precipitation and runoff records and sunspots may be coincidental and no clear evidence is
420 present of a direct cause-effect relationship.

421 Also the wavelet coherence spectra of precipitation and runoff (deseasonalized and not
422 deseasonalized) and the climate indexes considered in this paper, generally, do not highlight
423 clear results. The main findings seem to be:

- 424 • an area of significant coherence between precipitation and the NAO index at the 11–17
425 year band during the period 1880–1955 (Figure 15). The downward pointing arrows
426 suggest however a possible lead of one half of the respective time scale of 11 years, i.e.
427 about 5.5 years, of one against the other, which is somewhat difficult to explain physically;
- 428 • an area of significant coherence between precipitation and the AMO index at the 15–30
429 year scale band during the period 1920–1985 (Figure S6 in the supplementary material).

430 Moreover, some other sparse significant phase coherences at various scales are observed but
431 since they are not consistent, they may be considered spurious.

432 **4 Discussion and Conclusions**

433 We intend to discuss here the possible reasons of the observed significant negative trend of
434 runoff and of the runoff coefficient, pointed out in the statistics of Table 1, in Figures 6 and
435 7 and shown also in Figure 10 of the companion paper by Crespi et al. (this issue).

436 A possible explanation can be derived from Figure 16 showing the mean annual temperature
437 estimated as areal average over the basin and derived from a 30-arc second gridded dataset
438 of monthly temperature covering the study domain (Brunetti et al., 2006; Brunetti et al., 2009;
439 Brunetti et al., 2014). The linear regression line has a slope of $+1.1\text{ }^{\circ}\text{C century}^{-1}$, a value which
440 is consistent with the temperature trends in the Alpine region reported by several authors as
441 Böhm et al. (2001), Auer et al. (2007) and Brunetti et al. (2009). The same figure shows the
442 mean areal potential evapotranspiration (PET) estimated with the Thornthwaite method

443 computed on the same grid and then spatially averaged. It can be compared with annual water
444 losses estimated as the difference of corrected precipitation and runoff, thus neglecting the
445 effect of water storage in artificial reservoirs, lakes, groundwater, snow and glaciers. The
446 corrected precipitation record we use here (see Crespi et al., this issue) takes into account the
447 underestimation of solid precipitation which is known to be relevant in mountain areas
448 (Sevruk et al., 2009) and specifically in the investigated area (Eccel et al., 2012; Grossi et al.,
449 2017). The assumption that water storage is not relevant for this estimation is reasonable as
450 the change of these storage volumes at annual scale can be neglected with the exception of
451 glaciers which experienced a significant retreat that in the last three decades accelerated with
452 a volume loss of 12 mm yr^{-1} , as already discussed in Crespi et al. (this issue), providing an
453 additional contribution to runoff.

454 Part of the discrepancy between PET and the estimated annual losses is due to the fact that
455 actual evapotranspiration is less than the potential one. However, it is worth noticing that
456 observed losses increase in time, with a rate of $92 \text{ mm century}^{-1}$, much more rapidly than
457 PET estimates which show an increasing trend of $36 \text{ mm century}^{-1}$. The higher trend of
458 observed losses could be partly explained by the increased water exploitation for irrigation,
459 civil water supply and services. But it is also a result of the enhanced evapotranspiration
460 losses from forested areas which in Europe and the Alps expanded their extent because of
461 natural afforestation (FAO, 2018) as observed by Ranzi et al. (2017) in the nearby Adige
462 basin. This conjecture could be supported by further investigations including the analysis of
463 long-term land use changes and simulation of actual evapotranspiration losses.

464 In summary, the time series of the Lake Como daily inflow and outflow runoff reconstructed
465 for the 1845–2016 period, compared with contemporary monthly precipitation and
466 temperature observations and estimated PET losses, provides new data for a better insight
467 into the driving factors of the hydrological cycle in mountain areas over long-time scales. A
468 5 % significant decreasing trend of $-136 \text{ mm century}^{-1}$ was observed for annual runoff, to be
469 compared to the much lower non-significant trend $-41 \text{ mm century}^{-1}$ of annual uncorrected
470 precipitation (Crespi et al., this issue). The changes in runoff regime cannot be explained by
471 climatic changes alone and other factors influence several aspects of the observed variability.

472 Annual daily runoff maxima exhibit a decreasing trend, although not statistically significant,
473 with lower values after the mid-20th century when the hydropower reservoirs were close to
474 be completed. This could be partly explained by the fact that extreme flood volumes could
475 be stored in the reservoirs thus reducing the peak intensity.

476 The observed significant increase of annual 7-day runoff minima is likely a result of the
477 upstream reservoirs management practices that increase the hydropower generation in winter,
478 when the natural runoff regime exhibits its minima. The impact of water management
479 practice on the runoff record is also highlighted by the multi-scale spectral analysis conducted
480 by the wavelet transform. It indicates, in fact, an increasing trend of high-frequency energy
481 in both the daily inflow and outflow time series, observed especially after the completion of
482 the upstream hydropower reservoirs and the start of the Olginate barrage regulation at the
483 Lake Como outlet.

484 At larger time scales the wavelet analysis allows to point out the drought period of both
485 precipitation and runoff observed in the first decade of the 2000s and the long-term decrease
486 of runoff. However, this analysis does not support a solar signature in the precipitation and
487 runoff records. Our results, therefore, do not confirm the conclusions of Zanchettin et al.
488 (2008b) who suggest the influence of the solar activity on runoff records for the Po river.
489 Also the phase coherence of Adda catchment precipitation and runoff with the climate
490 indexes considered in the paper turns out to be rather low and it does not highlight clear
491 cause-effect relationships.

492 **Acknowledgments, Samples, and Data**

493 Luigi Bertoli from Consorzio dell'Adda is gratefully thanked for his valuable contribution to
494 the data collection and the authorisation to publish the results of the research conducted in
495 collaboration. The wavelet spectral analysis made use of the software developed by
496 C. Torrence and G. Compo freely available at <http://paos.colorado.edu/research/wavelets/>
497 and, for the coherence spectra, by A. Grinsted, J. Moore and S. Jevrejeva at
498 <http://grinsted.github.io/wavelet-coherence/>. Milan University activities have been
499 performed within IPCC MOUPA (Interdisciplinary Project for assessing current and
500 expected Climate Change impacts on MOUNTAIN PASTURES), developed within the AGER
501 Project, funded by Fondazione Cariplo. We dedicate this work to Baldassare Bacchi, who

502 provided his comments in the first stage of this study and for having taught the value of data
503 in hydrological research.

504 **References**

- 505 Auer, I. , Böhm, R. , Jurkovic, A. , Lipa, W. , Orlik, A. , Potzmann, R. , Schöner, W. ,
506 Ungersböck, M. , Matulla, C. , Briffa, K. , Jones, P. , Efthymiadis, D. , Brunetti, M. , Nanni,
507 T. , Maugeri, M. , Mercalli, L. , Mestre, O. , Moisselin, J. , Begert, M. , Müller-Westermeier,
508 G. , Kveton, V. , Bochnicek, O. , Stastny, P. , Lapin, M. , Szalai, S. , Szentimrey, T. , Cegnar,
509 T. , Dolinar, M. , Gajic-Capka, M. , Zaninovic, K. , Majstorovic, Z. and Nieplova, E. (2007),
510 HISTALP—historical instrumental climatological surface time series of the Greater Alpine
511 Region. *International Journal of Climatology*, 27: 17-46. <https://doi.org/10.1002/joc.1377>
- 512 Blöschl, G., Hall, J., Parajka, J., Perdigão, R. A., Merz, B., Arheimer, B., Aronica, G.T.,
513 Bilibashi, A., Bonacci, O., Borga, M., Čanjevac, I., Castellarin, A., Chirico, G. B., Claps, P.,
514 Fiala K., Frolova, N., Gorbachova, L., Gül, A., Hannaford, J., Harrigan, S., Kireeva, M.,
515 Kiss, A., Kjeldsen, T. R., Kohnová, S., Koskela, J.J., Ledvinka, O., Macdonald, N., Mavrova-
516 Guirguinova, M., Mediero, L., Merz, R., Molnar, P., Montanari, A., Murphy, C., Osuch, M.,
517 Ovcharuk, V., Radevski, I., Rogger, M., Salinas, J.L., Sauquet, E., Šraj, M., Szolgay, J.,
518 Viglione, A., Volpi, E., Wilson, D., Zaimi, K. and Živković, N. (2017), Changing climate
519 shifts timing of European floods. *Science*, 357(6351), 588-590.
520 <https://doi.org/10.1126/science.aan2506>
- 521 Böhm, R., Auer, I., Brunetti, M., Maugeri, M., Nanni, T. and Schöner, W. (2001). Regional
522 temperature variability in the European Alps: 1760–1998 from homogenized instrumental
523 time series. *International Journal of Climatology*, 21(14), 1779-1801.
524 <https://doi.org/10.1002/joc.689>
- 525 Brugnara, Y. and Maugeri, M. (2019). Daily precipitation variability in the southern Alps
526 since the late 19th century. *International Journal of Climatology*. 39(8), 3492-3504.
527 <https://doi.org/10.1002/joc.6034>
- 528 Brunetti, M., Maugeri, M., Nanni, T., Simolo, C. and Spinoni, J. (2014). High-resolution
529 temperature climatology for Italy: interpolation method intercomparison. *International*
530 *Journal of Climatology*, 34, 1278–1296. <https://doi.org/10.1002/joc.3764>

531 Brunetti, M., Lentini, G., Maugeri, M., Nanni, T., Auer, I., Böhm, R. and Schöner, W. (2009),
532 Climate variability and change in the Greater Alpine Region over the last two centuries based
533 on multi-variable analysis. *International Journal of Climatology*, 29(15), 2197–2225.
534 <https://doi.org/10.1002/joc.1857>

535 Brunetti M, Maugeri M, Monti F and Nanni T (2006b). Temperature and precipitation
536 variability in Italy in the last two centuries from homogenised instrumental time series.
537 *International Journal of Climatology* 26: 345–381. <https://doi.org/10.1002/joc.1251>

538 Carey S. K., Tetzlaff D., Buttle J., Laudon H., McDonnell J., McGuire K. and Shanley, J.
539 (2013) Use of color maps and wavelet coherence to discern seasonal and interannual climate
540 influences on streamflow variability in northern catchments. *Water Resources Research*,
541 49(10), 6194-6207. <https://doi.org/10.1002/wrcr.20469>

542 Citrini, D. (1977), *Le piene del Lario e dell’Adda nel regime regolato*, Milano, Consorzio
543 dell’Adda, Pubblicazione n. 10.

544 Consorzio dell’Adda. (1958) *La regolazione del Lago di Como nel primo decennio di*
545 *esercizio 1946-1955*, Milano.

546 Coulibaly P. and Burn, D. H. (2004). Wavelet analysis of variability in annual Canadian
547 streamflows. *Water Resources Research*, 40(3). <https://doi.org/10.1029/2003WR002667>

548 Crespi A., Brunetti M., Ranzi R., Tomirotti M. and Maugeri M. (2019). A multi-century
549 meteo-hydrological analysis for the Adda river basin (Central Alps). Part I: gridded monthly
550 precipitation (1800-2016) records. *International Journal of Climatology*, (this issue,
551 submitted).

552 D’Agata, C., Bocchiola, D., Soncini, A., Maragno, D., Smiraglia, C. and Diolaiuti, G. A.
553 (2018). Recent area and volume loss of Alpine glaciers in the Adda River of Italy and their
554 contribution to hydropower production. *Cold Regions Science and Technology*, 148, 172–
555 184. <https://doi.org/10.1016/j.coldregions.2017.12.010>

556 Daubechies, I. (1990). The wavelet transform, time-frequency localization and signal
557 analysis. *IEEE transactions on information theory*, 36(5), 961-1005.
558 <https://doi.org/10.1109/18.57199>

559 De Marchi, G. (1970). *La regolazione del lago di Como nei sei anni dal 1963 al 1968*, Milano,
560 Consorzio dell’Adda, Pubblicazione n. 8.

561 Dong, L., Fu, C., Liu, J. and Zhang, P. (2018). Combined Effects of Solar Activity and El
562 Niño on Hydrologic Patterns in the Yoshino River Basin, Japan. *Water Resources*
563 *Management*, 32(7), 2421-2435. <https://doi.org/10.1007/s11269-018-1937-1>

564 Eccel, E., Cau, P., and Ranzi, R. (2012). Data reconstruction and homogenization for
565 reducing uncertainties in high-resolution climate analysis in Alpine regions. *Theoretical and*
566 *Applied Climatology*, 110(3), 345-358. <https://doi.org/10.1007/s00704-012-0624-z>

567 FAO (2018). State of the World's Forests 2018 - Forest pathways to sustainable development.
568 Rome.

569 Grinsted, A., Moore, J. C. and Jevrejeva, S. (2004). Application of the cross wavelet
570 transform and wavelet coherence to geophysical time series. *Nonlinear Processes in*
571 *Geophysics*, 11(5/6), 561-566. <https://doi.org/10.5194/npg-11-561-2004>

572 Grossi, G., Lendvai, A., Peretti, G., and Ranzi, R. (2017). Snow precipitation measured by
573 gauges: Systematic error estimation and data series correction in the central Italian Alps.
574 *Water*, 9(7), 461. <https://doi.org/10.3390/w9070461>

575 IPCC (2013), Summary for Policymakers. In: Climate Change 2013: The Physical Science
576 Basis. Contribution of Working Group I to the Fifth Assessment Report of the
577 Intergovernmental Panel on Climate Change [Stocker, T.F., D. Qin, G.-K. Plattner, M.
578 Tignor, S. K. Allen, J. Boschung, A. Nauels, Y. Xia, V. Bex and P.M. Midgley (eds.)].
579 Cambridge University Press, Cambridge, United Kingdom and New York, NY, USA.
580 <https://doi.org/10.1017/CBO9781107415324>

581 IPCC (2014) Summary for Policymakers. In: Climate Change 2014: Mitigation of Climate
582 Change. Contribution of Working Group III to the Fifth Assessment Report of the
583 Intergovernmental Panel on Climate Change [Edenhofer, O., R. Pichs-Madruga, Y. Sokona,
584 E. Farahani, S. Kadner, K. Seyboth, A. Adler, I. Baum, S. Brunner, P. Eickemeier, B.
585 Kriemann, J. Savolainen, S. Schlömer, C. von Stechow, T. Zwickel and J.C. Minx (eds.)].
586 Cambridge University Press, Cambridge, United Kingdom and New York, NY, USA.
587 <https://doi.org/10.1017/cbo9781107415416.005>

588 Jevrejeva, S., Grinsted, A., Moore, J. C. and Holgate, S. (2006). Nonlinear trends and
589 multiyear cycles in sea level records. *Journal of Geophysical Research: Oceans*, 111(C9).
590 <https://doi.org/10.1029/2005JC003229>

591 Jones, P.D., Jónsson, T. and Wheeler, D. (1997). Extension to the North Atlantic Oscillation
592 using early instrumental pressure observations from Gibraltar and South-West Iceland.
593 *International Journal of Climatology*, 17(13), 1433-1450.
594 [https://doi.org/10.1002/\(SICI\)1097-0088\(19971115\)17:13<1433::AID-JOC203>3.0.CO;2-](https://doi.org/10.1002/(SICI)1097-0088(19971115)17:13<1433::AID-JOC203>3.0.CO;2-)
595 [P](#)

596 Kendall, M.G. (1975). Rank Correlation Methods. Charles Griffin, London.
597 doi:10.2307/2333282

598 Küçük, M., Kahya, E., Cengiz, T. M. and Karaca, M. (2009). North Atlantic Oscillation
599 influences on Turkish lake levels. *Hydrological Processes*, 23(6), 893-906.
600 <https://doi.org/10.1002/hyp.7225>

601 Kumar, P. and Foufoula-Georgiou, E. (1993). A multicomponent decomposition of spatial
602 rainfall fields: 1. Segregation of large-and small-scale features using wavelet transforms.
603 *Water Resources Research*, 29(8), 2515-2532. <https://doi.org/10.1029/93WR00548>

604 Labat, D., Ababou, R. and Mangin, A. (2000). Rainfall–runoff relations for karstic springs.
605 Part II: continuous wavelet and discrete orthogonal multiresolution analyses. *Journal of*
606 *Hydrology*, 238(3-4), 149-178. [https://doi.org/10.1016/S0022-1694\(00\)00322-X](https://doi.org/10.1016/S0022-1694(00)00322-X)

607 Labat, D., Ronchail, J. and Guyot, J. L. (2005). Recent advances in wavelet analyses: Part 2-
608 Amazon, Parana, Orinoco and Congo discharges time scale variability. *Journal of*
609 *Hydrology*, 314(1-4), 289-311. <https://doi.org/10.1016/j.jhydrol.2005.04.004>

610 Lombardini, E. (1866). Della natura dei laghi, 2nd edition, Tipografia degli ingegneri,
611 Milano.

612 López-Moreno, J. I., Vicente-Serrano, S. M., Morán-Tejeda, E., Lorenzo-Lacruz, J.,
613 Kenawy, A. and Beniston, M. (2011). Effects of the North Atlantic Oscillation (NAO) on
614 combined temperature and precipitation winter modes in the Mediterranean mountains:
615 observed relationships and projections for the 21st century. *Global and Planetary Change*,
616 77(1-2), 62-76. <https://doi.org/10.1016/j.gloplacha.2011.03.003>

617 Malusardi, G. and Moissello, U. (2003), Gli effetti della regolazione sulle portate dell'Adda e
618 sulle piene del lago di Como, Consorzio dell'Adda, pubblicazione n. 13, Milano.

619 Marazzi, A., Gamba, P. and Ranzi, R. (1996). Rain pattern detection by means of packet
620 wavelets. In IGARSS'96. 1996 International Geoscience and Remote Sensing Symposium
621 (Vol. 1, pp. 266-268). IEEE. <https://doi.org/10.1109/IGARSS.1996.516312>

622 Markovic, D. and Koch, M. (2005). Wavelet and scaling analysis of monthly precipitation
623 extremes in Germany in the 20th century: Interannual to interdecadal oscillations and the
624 North Atlantic Oscillation influence. *Water Resources Research*, 41(9).
625 <https://doi.org/10.1029/2004WR003843>

626 Martin-Vide, J. and Lopez-Bustins, J. A. (2006). The western Mediterranean oscillation and
627 rainfall in the Iberian Peninsula. *International Journal of Climatology*, 26(11), 1455-1475.
628 <https://doi.org/10.1002/joc.1388>

629 Milly, P. C., Betancourt, J., Falkenmark, M., Hirsch, R. M., Kundzewicz, Z. W., Lettenmaier,
630 D. P. and Stouffer, R. J. (2008). Stationarity is dead: Whither water management?. *Science*,
631 319(5863), 573-574. <https://doi.org/10.1126/science.1151915>

632 Moisello, U. and Vullo, F. (2009), I massimi di portata dell'Adda a Lecco, l'Acqua, 6, 9-27.

633 Montanari, A. (2012), Hydrology of the Po River: looking for changing patterns in river
634 discharge, *Hydrology and Earth System Sciences*, 16(10), 3739-3747.
635 <https://doi.org/10.5194/hess-16-3739-2012>

636 Montanari, A. and Koutsoyiannis, D. (2014). Modeling and mitigating natural hazards:
637 Stationarity is immortal!. *Water Resources Research*, 50(12), 9748-9756.
638 <https://doi.org/10.1002/2014WR016092>

639 Moore, J., Grinsted, A. and Jevrejeva, S. (2006). Is there evidence for sunspot forcing of
640 climate at multi-year and decadal periods?. *Geophysical Research Letters*, 33(17).
641 <https://doi.org/10.1029/2006GL026501>

642 Nakken, M. (1999). Wavelet analysis of rainfall–runoff variability isolating climatic from
643 anthropogenic patterns. *Environmental Modelling & Software*, 14(4), 283-295.
644 [https://doi.org/10.1016/S1364-8152\(98\)00080-2](https://doi.org/10.1016/S1364-8152(98)00080-2)

645 Osborn T. J. (2011). Winter 2009/2010 temperatures and a record-breaking North Atlantic
646 Oscillation index. *Weather*, 66(1), 19-21. <https://doi.org/10.1002/wea.660>

647 Ranzi, R., Caronna, P. and Tomirotti, M. (2017). Impact of climatic and land use changes on
648 river flows in the Southern Alps. In Sustainable Water Resources Planning and Management

649 Under Climate Change (pp. 61-83). Springer, Singapore. [https://doi.org/10.1007/978-981-](https://doi.org/10.1007/978-981-10-2051-3_3)
650 [10-2051-3_3](https://doi.org/10.1007/978-981-10-2051-3_3)

651 Ranzi, R., Bacchi, B., Tomirotti, M., Castioni, C., Brunetti, M., Crespi, A. and Maugeri, M.
652 (2018a), Analisi delle tendenze di lungo termine nel regime degli afflussi meteorici e dei
653 deflussi dell'Adda a Lecco (1845-2014), *L'Acqua*, 2, 51-60.

654 Ranzi, R., Bacchi, B., Castioni, C., Michailidi, E. M., Tomirotti, M. and Bertoli, L. (2018b),
655 Livelli idrometrici, afflussi e deflussi giornalieri del Lago di Como nel periodo 1845-2016,
656 Consorzio dell'Adda, Milano, Pubblicazione n. 14, 2018.

657 Rodriguez-Iturbe, I. and Yevjevich, V. M. (1968). The investigation of relationship between
658 hydrologic time series and sunspot numbers. *Hydrology papers (Colorado State University)*;
659 no. 26.

660 Rossi, A., Massei, N., Laignel, B., Sebag, D. and Copard, Y. (2009). The response of the
661 Mississippi River to climate fluctuations and reservoir construction as indicated by wavelet
662 analysis of streamflow and suspended-sediment load, 1950–1975. *Journal of Hydrology*,
663 377(3-4), 237-244. <https://doi.org/10.1016/j.jhydrol.2009.08.032>

664 Salvatore, M.C., Zanoner, T., Baroni, C., Carton, A., Banchieri, F.A., Viani C., Giardino M.
665 and Perotti L. (2015). The state of Italian glaciers: a snapshot of the 2006-2007 hydrological
666 period, *Geografia Fisica e Dinamica Quaternaria*, 38(2), 175-198.
667 <https://doi.org/10.4461/GFDQ.2015.38.16>

668 Sen, P.K. (1968). Estimates of the regression coefficient based on Kendall's tau. *Journal of*
669 *the American Statistical Association*, 63(324), 1379-1389. <https://doi.org/10.2307/2285891>

670 Shorthouse, C. and Arnell, N. (1999). The effects of climatic variability on spatial
671 characteristics of European river flows. *Physics and Chemistry of the Earth, Part B:*
672 *Hydrology, Oceans and Atmosphere*, 24(1-2), 7-13. [https://doi.org/10.1016/S1464-](https://doi.org/10.1016/S1464-1909(98)00003-3)
673 [1909\(98\)00003-3](https://doi.org/10.1016/S1464-1909(98)00003-3)

674 Smiraglia C. and Diolaiuti G. (eds.) (2015). *Il Nuovo Catasto dei Ghiacciai Italiani*. Ev-K2-
675 CNR Ed., Bergamo.

676 Smith, L. C., Turcotte, D. L. and Isacks, B. L. (1998). Stream flow characterization and
677 feature detection using a discrete wavelet transform. *Hydrological Processes*, 12(2), 233-

678 249. [https://doi.org/10.1002/\(SICI\)1099-1085\(199802\)12:2<233::AID-HYP573>3.0.CO;2-](https://doi.org/10.1002/(SICI)1099-1085(199802)12:2<233::AID-HYP573>3.0.CO;2-3)
679 [3](https://doi.org/10.1002/(SICI)1099-1085(199802)12:2<233::AID-HYP573>3.0.CO;2-3)

680 Sneyers, R. (1992). On the use of statistical analysis for the objective determination of
681 climate change. *Meteorologische Zeitschrift*, 1(5), 247-256.
682 <https://doi.org/10.1127/metz/1/1992/247>

683 Stahl, K., Hisdal, H., Hannaford, J., Tallaksen, L., Van Lanen, H., Sauquet, E., Demuth, S.,
684 Fendekjova, M. and Jordar, J. (2010). Streamflow trends in Europe: evidence from a dataset
685 of near-natural catchments. *Hydrology and Earth System Sciences*, 14(12), 2367-2382.
686 <https://doi.org/10.5194/hess-14-2367-2010>

687 Steirou, E., Gerlitz, L., Apel, H. and Merz, B. (2017). Links between large-scale circulation
688 patterns and streamflow in Central Europe: A review. *Journal of Hydrology*, 549, 484-500.
689 <https://doi.org/10.1016/j.jhydrol.2017.04.003>

690 Su, L., Miao, C., Kong, D., Duan, Q., Lei, X., Hou, Q. and Li, H. (2018), Long-term trends
691 in global river flow and the causal relationships between river flow and ocean signals.
692 *Journal of Hydrology*, 563, 818-833. <https://doi.org/10.1016/j.jhydrol.2018.06.058>

693 Torrence, C. and Compo, G. P. (1998). A practical guide to wavelet analysis. *Bulletin of the*
694 *American Meteorological society*, 79(1), 61-78. [https://doi.org/10.1175/1520-](https://doi.org/10.1175/1520-0477(1998)079<0061:APGTWA>2.0.CO;2)
695 [0477\(1998\)079<0061:APGTWA>2.0.CO;2](https://doi.org/10.1175/1520-0477(1998)079<0061:APGTWA>2.0.CO;2)

696 Tsiropoula, G. (2003). Signatures of solar activity variability in meteorological parameters.
697 *Journal of Atmospheric and Solar-Terrestrial Physics*, 65(4), 469-482.
698 [https://doi.org/10.1016/S1364-6826\(02\)00295-X](https://doi.org/10.1016/S1364-6826(02)00295-X)

699 Wrzesiński, D. and Paluszkiewicz, R. (2011). Spatial differences in the impact of the North
700 Atlantic Oscillation on the flow of rivers in Europe. *Hydrology Research*, 42(1), 30-39.
701 <https://doi.org/10.2166/nh.2010.077>

702 Zampieri, M., Toreti, A., Schindler, A., Scoccimarro, E. and Gualdi, S. (2017). Atlantic
703 multi-decadal oscillation influence on weather regimes over Europe and the Mediterranean
704 in spring and summer. *Global and Planetary Change*, 151, 92-100.
705 <https://doi.org/10.1016/j.gloplacha.2016.08.014>

706 Zanchettin, D., Traverso, P. and Tomasino, M. (2008a). Po River discharge: a preliminary
 707 analysis of a 200-year time series, *Climatic Change*, 88(3), 411–433.
 708 <https://doi.org/10.1007/s10584-008-9395-z>

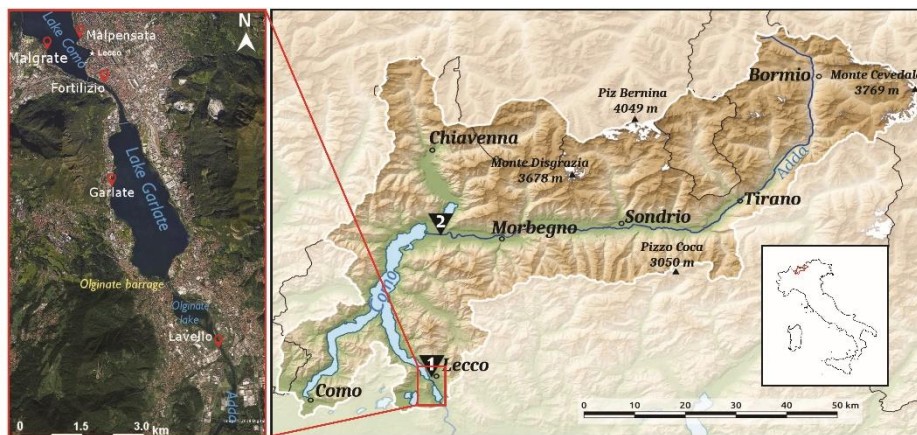
709 Zanchettin, D., Rubino, A., Traverso, P. and Tomasino, M. (2008b). Impact of variations in
 710 solar activity on hydrological decadal pattern in Northern Italy, *Journal of Geophysical*
 711 *Research*, 113, D12102. <https://doi.org/10.1029/2007JD009157>

712 Zanchettin, D., Rubino, A., Traverso, P. and Tomasino, M. (2009). Teleconnections force
 713 interannual-to-decadal tidal variability in the Lagoon of Venice (northern Adriatic). *Journal*
 714 *of Geophysical Research: Atmospheres*, 114(D7), D07106.
 715 <https://doi.org/10.1029/2008JD011485>

716 Zhang, Q., Singh, V. P., Li, K. and Li, J. (2014). Trend, periodicity and abrupt change in
 717 streamflow of the East River, the Pearl River basin. *Hydrological Processes*, 28(2), 305-314.
 718 <https://doi.org/10.1002/hyp.9576>

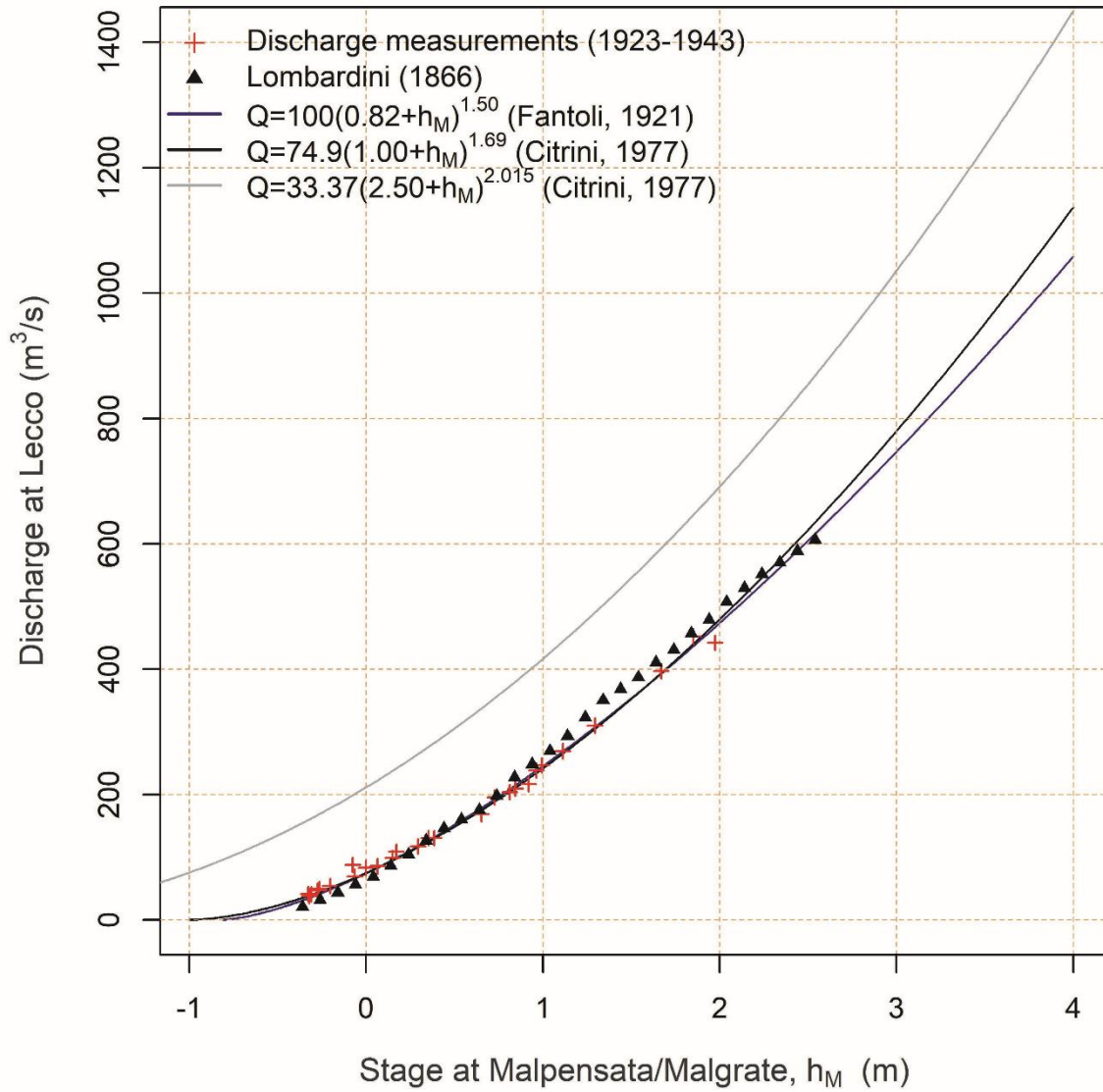
719 Zolezzi, G., Bellin, A., Bruno, M. C., Maiolini, B. and Siviglia, A. (2009). Assessing
 720 hydrological alterations at multiple temporal scales: Adige River, Italy. *Water Resources*
 721 *Research*, 45(12), W12421. <https://doi.org/10.1029/2008WR007266>

722 **Figures and Tables**

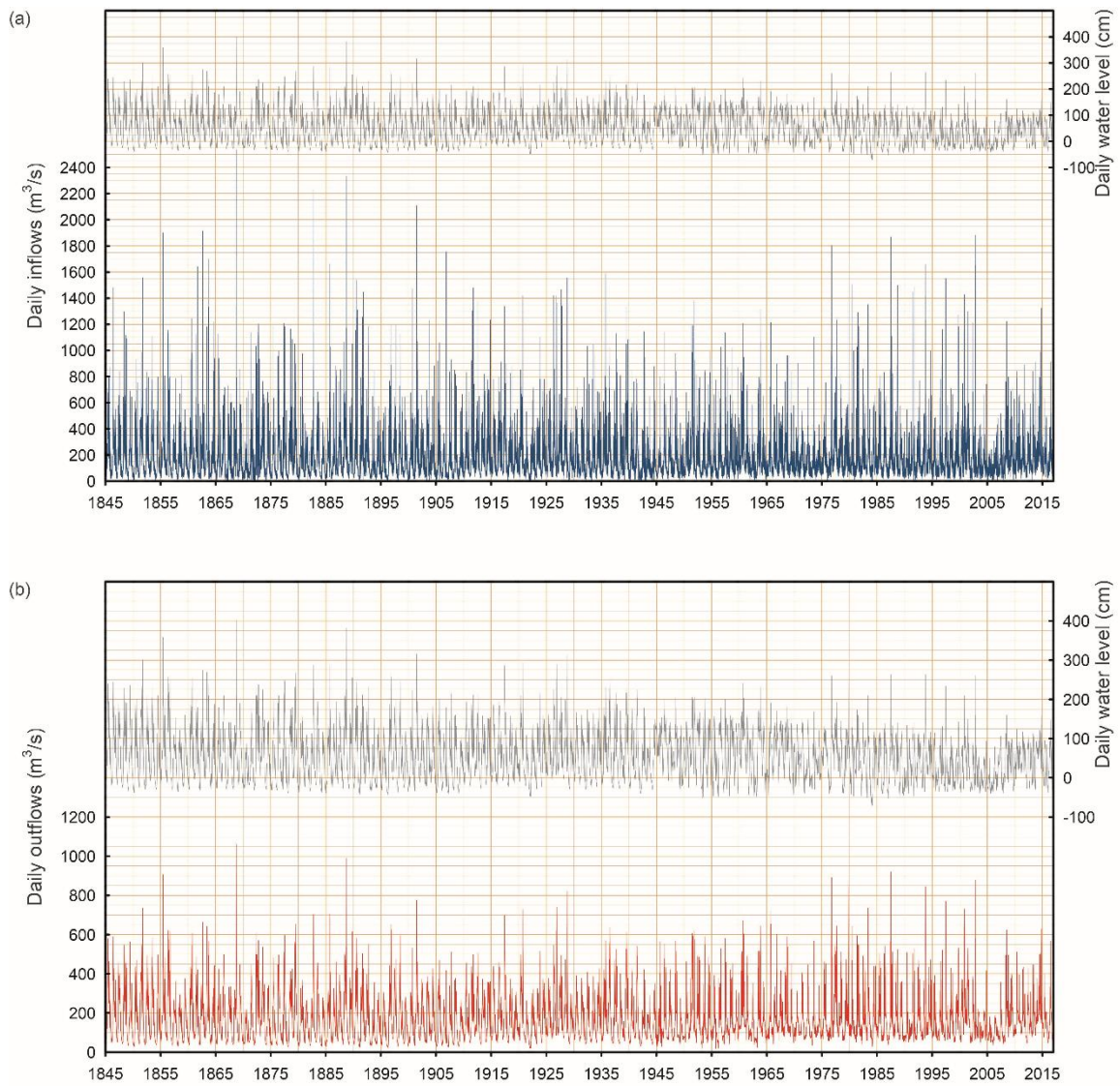


723 **Figure 1:** The Adda river basin with outlet at Lavello (right) and satellite imagery of the
 724 surroundings at the outlet (left). The figure shows also the position of the Fortilizio, close to
 725 Lecco, and Fuentes hydrometric stations, indicated by 1 and 2, respectively (Source: Google

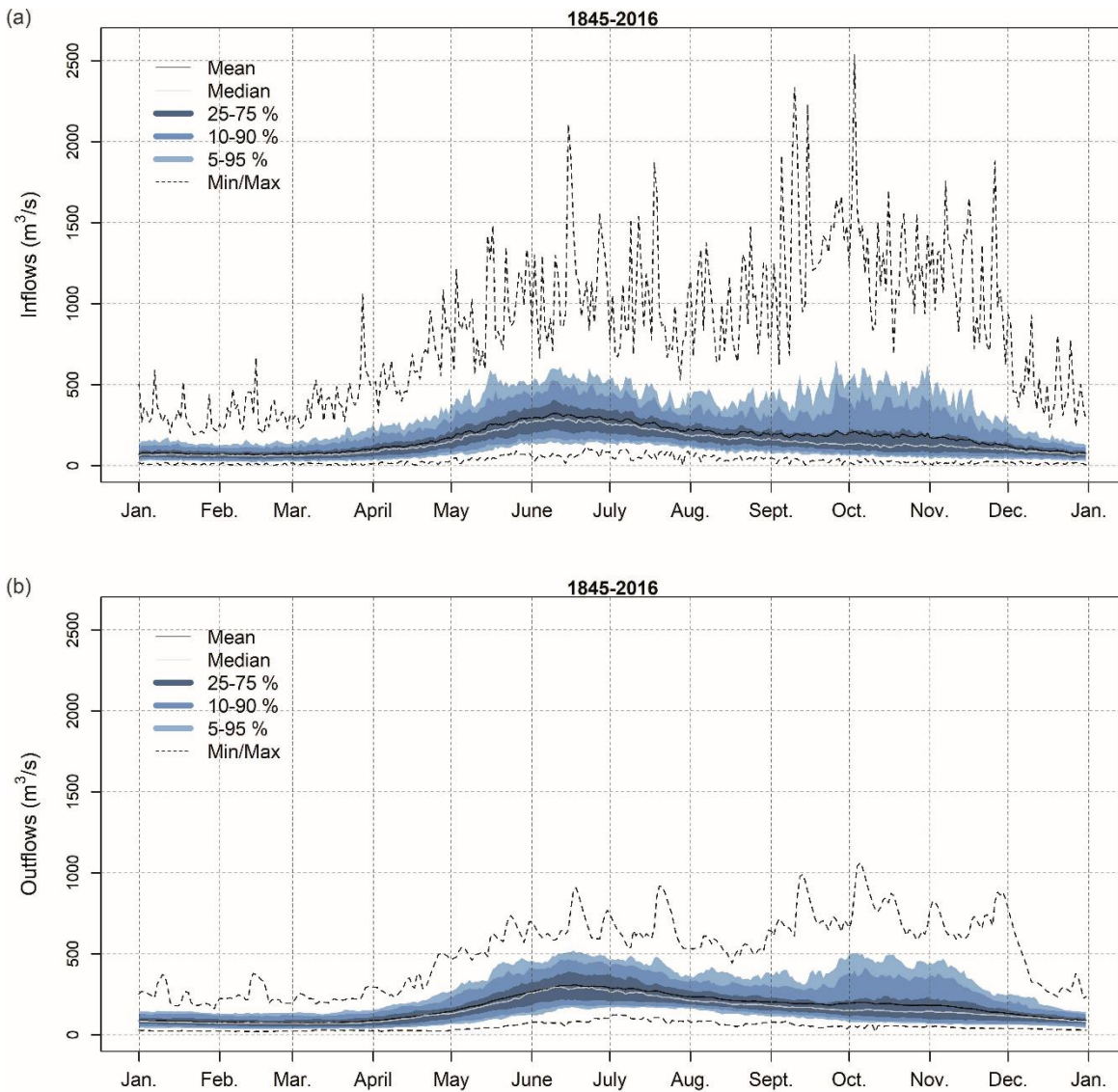
726 Earth. Lago di Como, Italia. 45°49'25" N 9°23'31" E, Elevation 14.11 km. DigitalGlobe
727 2018, 24 July, 2018).



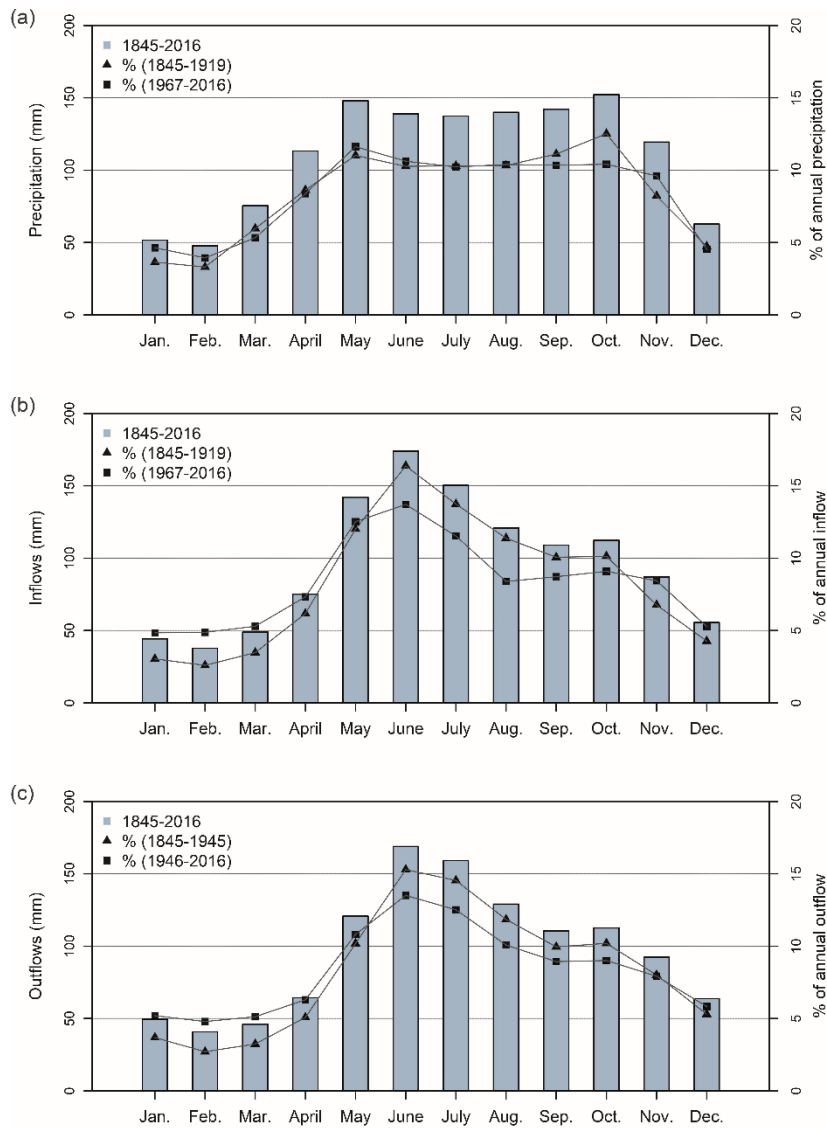
728 **Figure 2:** Pre- and post-regulation stage-discharge curves and comparison with discharge
729 measurements. The grey curve is valid for the post-regulation (1946–2016) period.



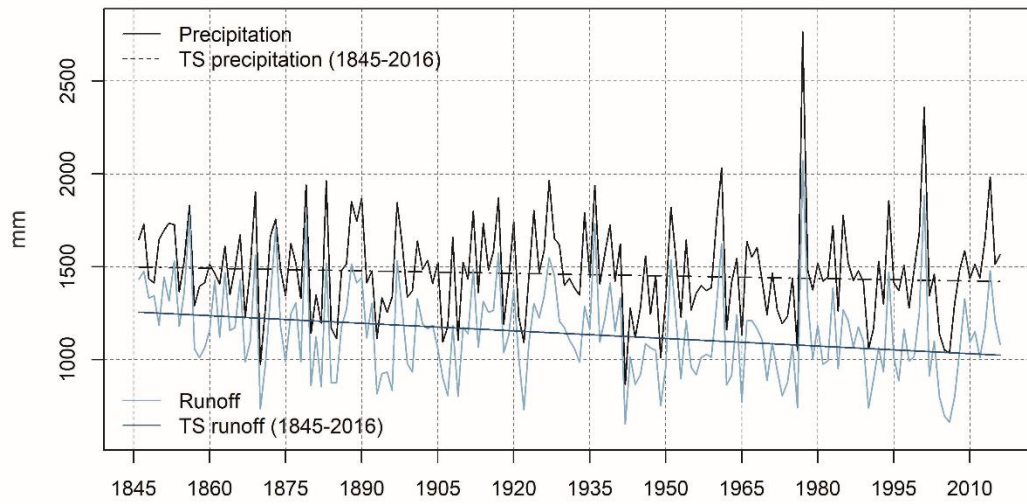
730 **Figure 3:** The daily Lake Como water level (grey) for the period 1845–2016, together with
 731 inflow (a) and outflow (b) series.



732 **Figure 4:** (a) Seasonal mean, median, maxima, minima, and 5, 10, 25 % upper and lower
 733 quantiles of Lake Como inflows in the 1845-2016 period. b) as for (a) but for Lake Como
 734 outflows.



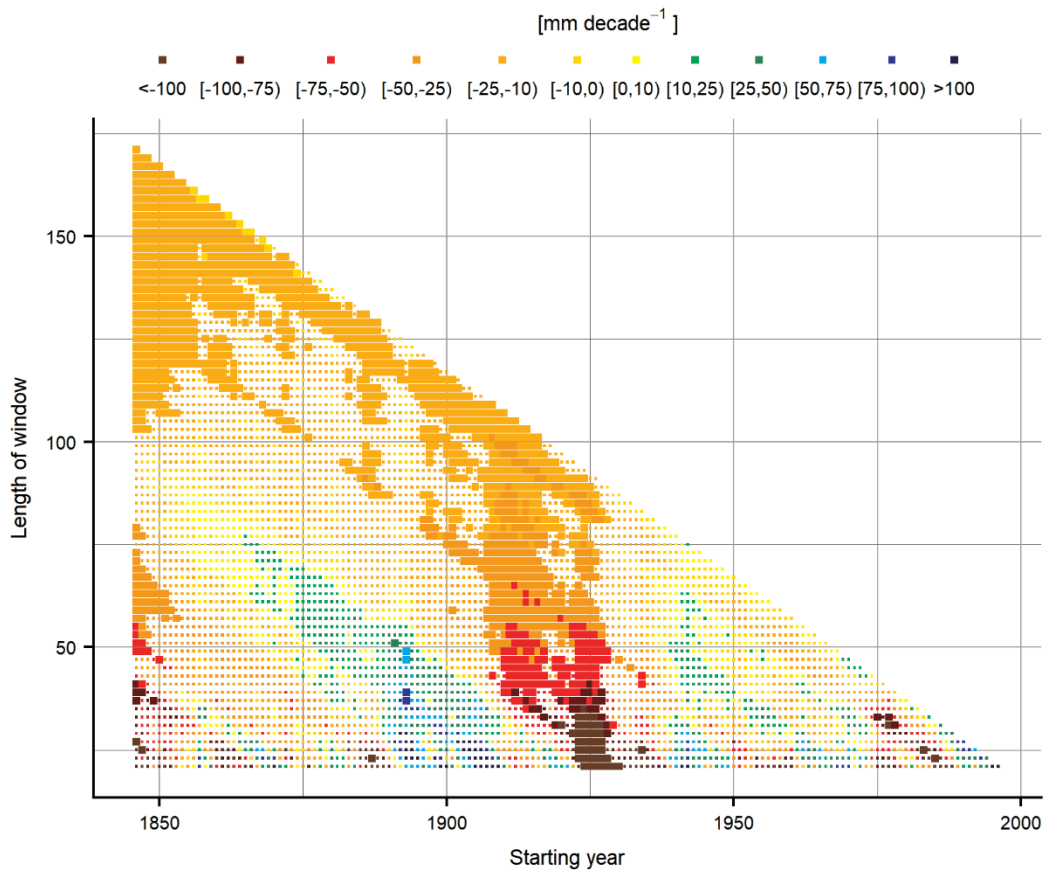
735 **Figure 5:** Yearly cycles of precipitation (a), Lake Como inflows (b) and Lake Como outflows
 736 (c) in the 1845-2016 period and relative contributions of each month to the corresponding
 737 yearly precipitation (a), Lake Como inflows (b) and Lake Como outflows (c). For
 738 precipitation and Lake Como inflows, the relative contributions are reported for the two
 739 periods 1845-1919 and 1967-2016, whereas for Lake Como outflows they are reported for
 740 the two periods 1845-1945 and 1946-2016 for the reasons described in the paper.



741 **Figure 6:** Theil-Sen trend of annual precipitation and annual runoff of the Adda river basin
 742 in the hydrological years starting with September 1845 until August 2016.

SERIES	PERIOD	Z_{MK}	THEIL-SEN	P-VALUE	95 % CONFID. INTERVAL
Inflow	1846–2016	-3.53	-136 mm century ⁻¹	0.00	[-210, -62] mm century ⁻¹
Runoff coefficient	1846–2016	-6.21	-0.06 century ⁻¹	0.00	[-0.08, -0.04] century ⁻¹

744 **Table 1.** Mann-Kendall Z statistic and Theil-Sen slope, along with p-values (significance in
745 bold) and 95 % confidence interval of the Theil-Sen slope for the annual runoff and runoff
746 coefficient of for the entire period (hydrological year)

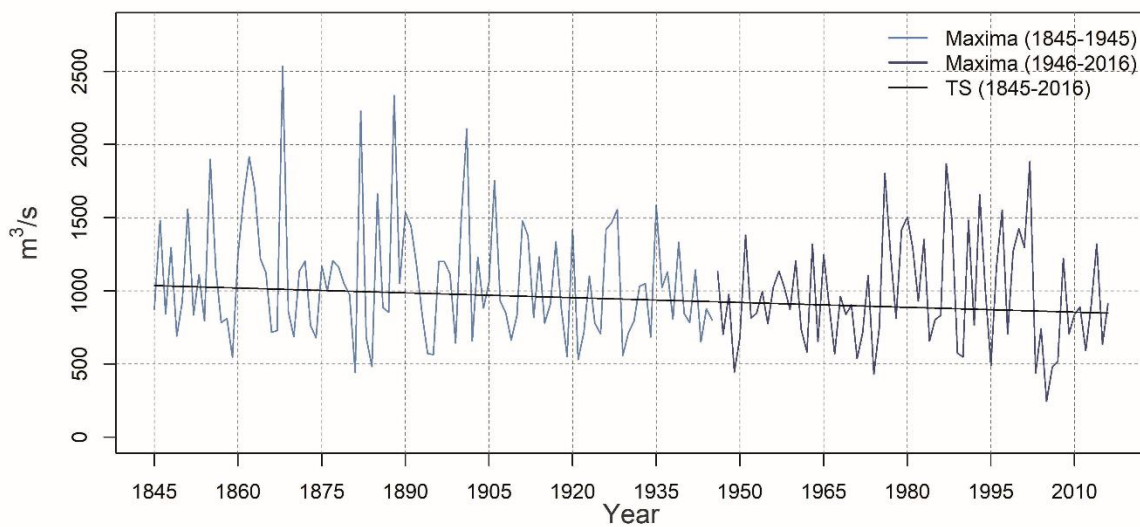


747 **Figure 7:** Running trend of annual inflow runoff. Trend values are expressed by colors while
748 the significance of trend is represented by the pixel size (larger pixels for Mann-Kendall p-
749 values < 0.05).

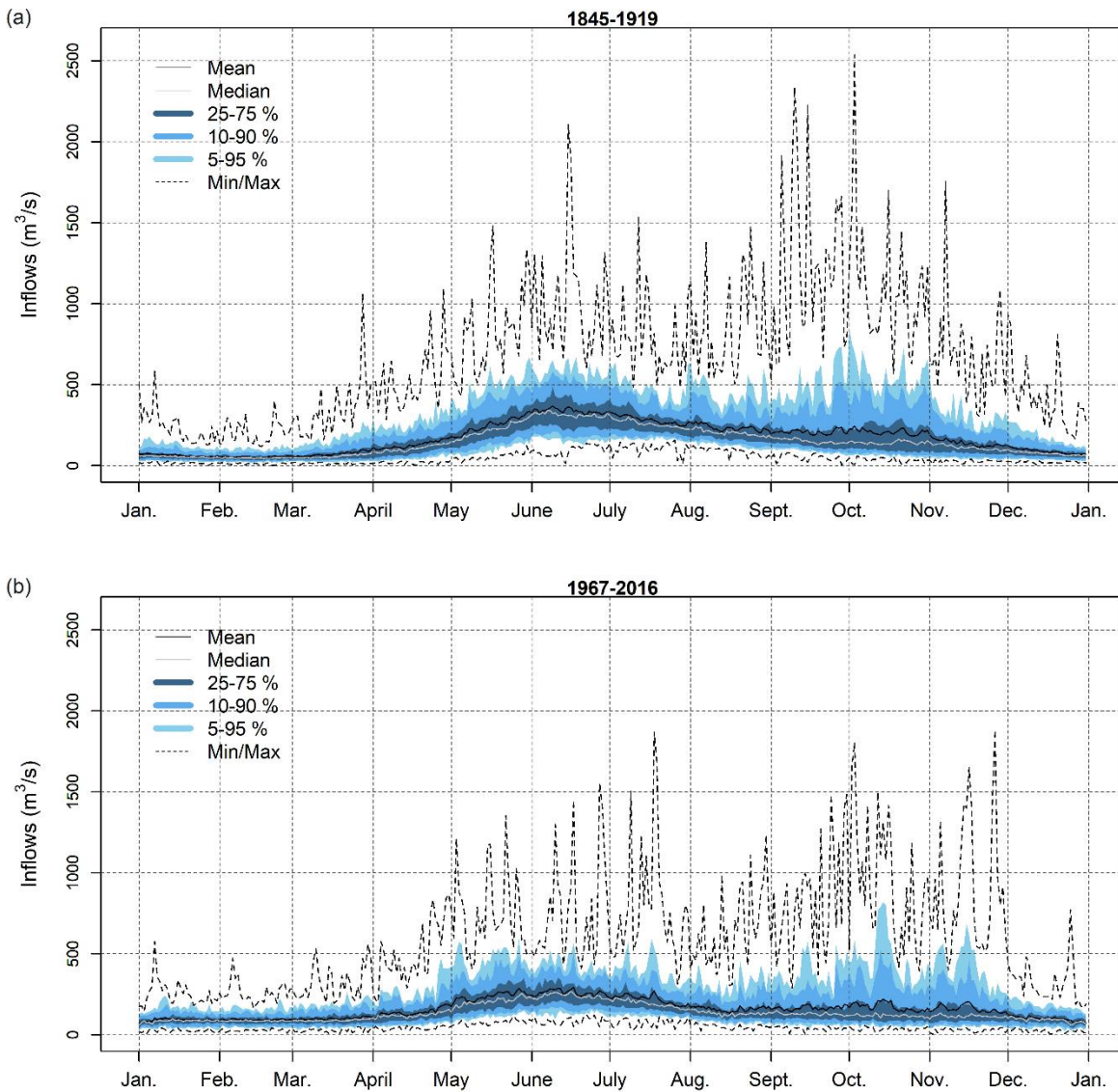
SERIES	PERIOD	Z _{MK}	THEIL-SEN (mm year ⁻¹)	P-VALUE	95 % CONFID. INTERVAL (mm year ⁻¹)
Maxima	1846–2016	-1.86	-1.10	0.06	[-2.21, 0.06]
Minima	1846–2016	-7.70	0.16	0.00	[0.13, 0.19]

751

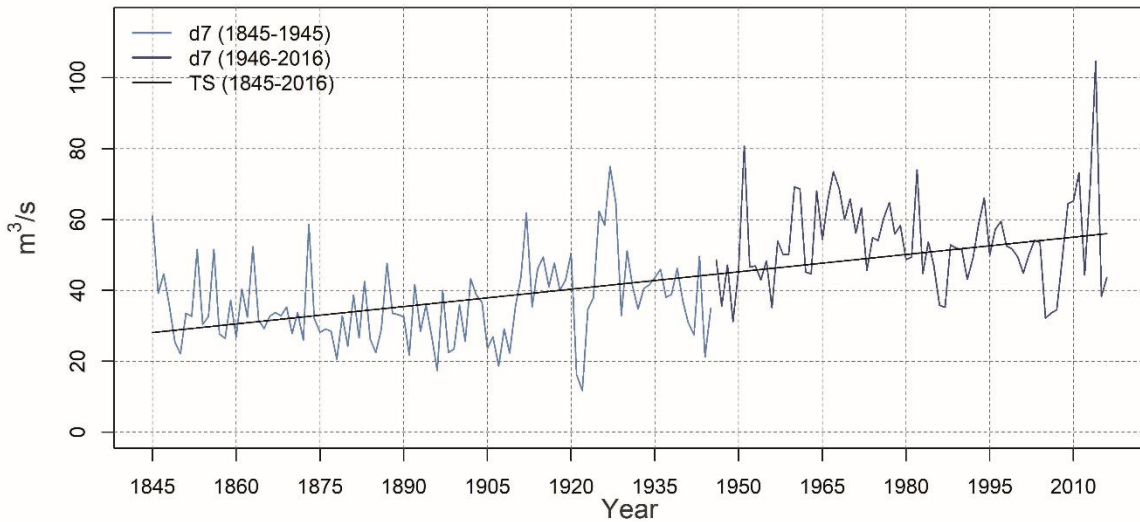
752 **Table 2.** Mann-Kendall Z statistic and Theil-Sen slope, along with p-values ($p < 0.05$ in bold)
753 and 95 % confidence interval of the Theil-Sen slope for the daily annual maximum and
754 annual 7-day minimum inflow.



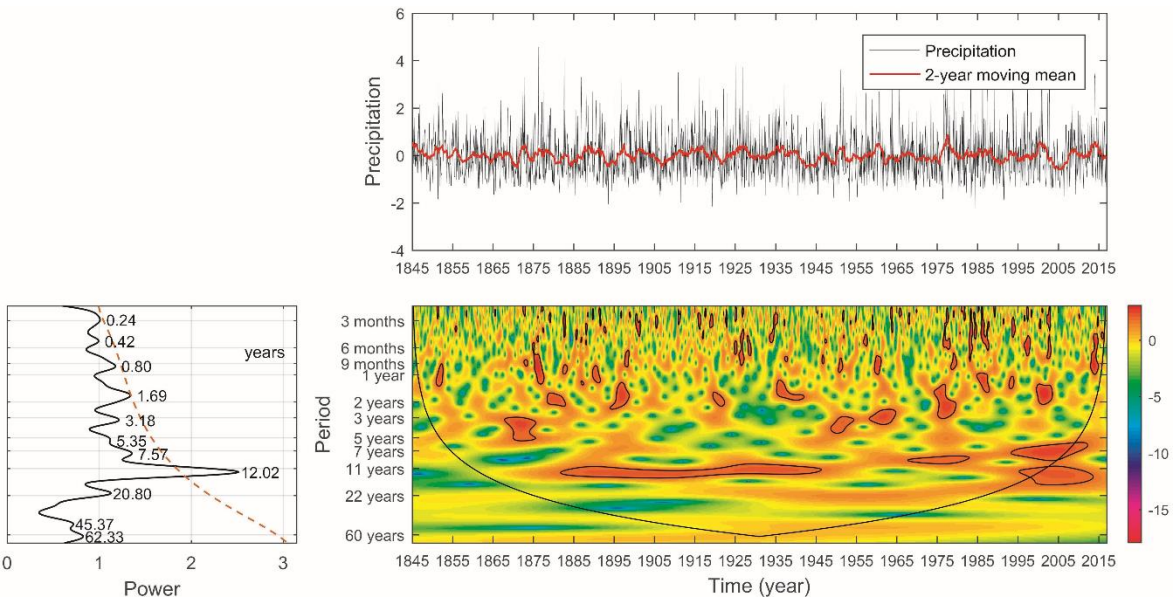
755 **Figure 8:** Theil-Sen trend of annual maxima daily inflow to Lake Como (Adda river basin).



756 **Figure 9:** Seasonal mean, median, maxima, minima, and 5, 10, 25 % upper and lower
 757 quantiles of Lake Como inflows in the 1845-1919 (a) and 1967-2016 periods (b).

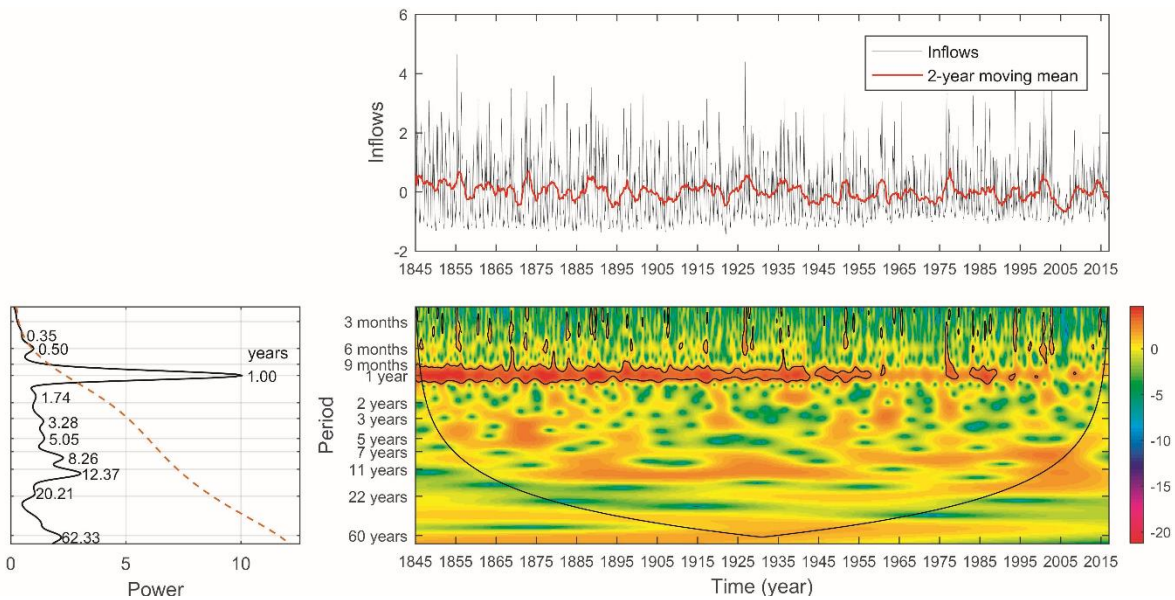


759 **Figure 10:** Theil-Sen trend of annual 7-day minimum inflow to Lake Como (Adda river
 760 basin).

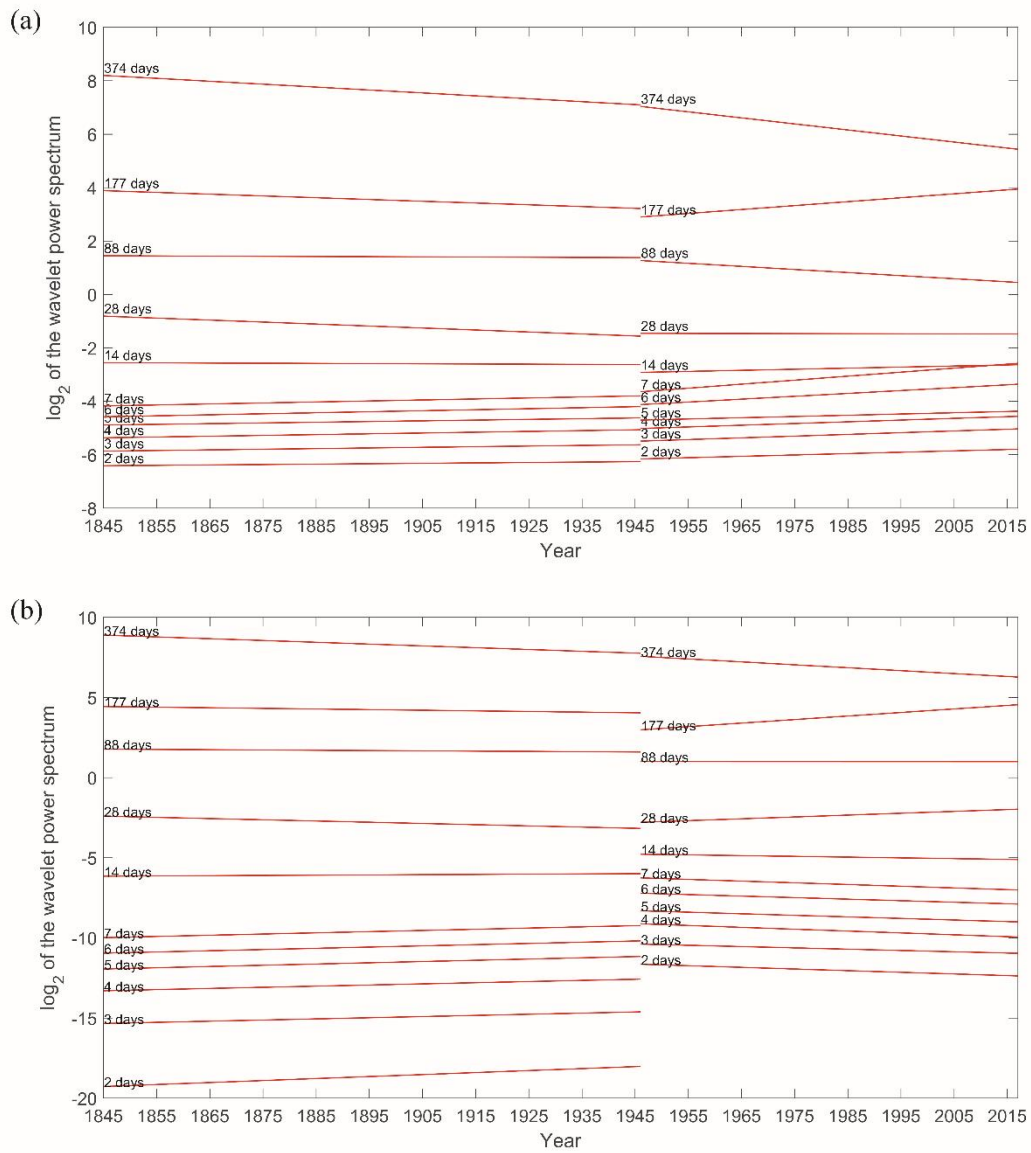


761

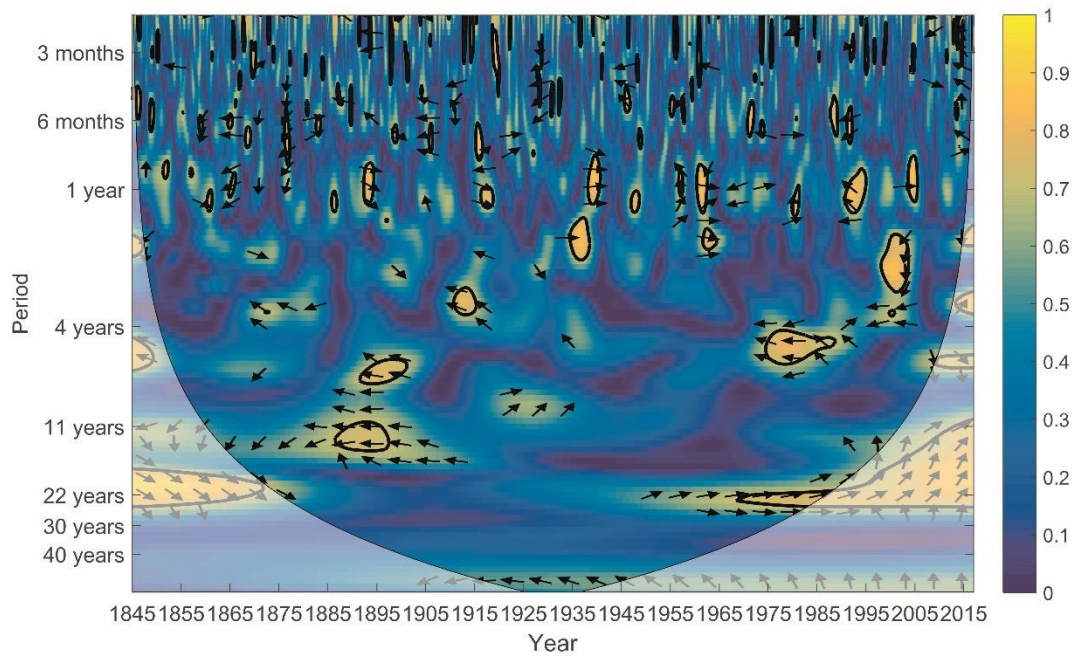
762 **Figure 11:** Time series, dimensionless wavelet spectrum (bottom right) and global wavelet
 763 spectrum (bottom left) of monthly precipitation (deseasonalized); 5% significance levels are
 764 marked with black contour lines in wavelet spectrum and COI-Cone Of Influence; in global
 765 wavelet spectrum 5% significance levels are marked with the dashed red line.



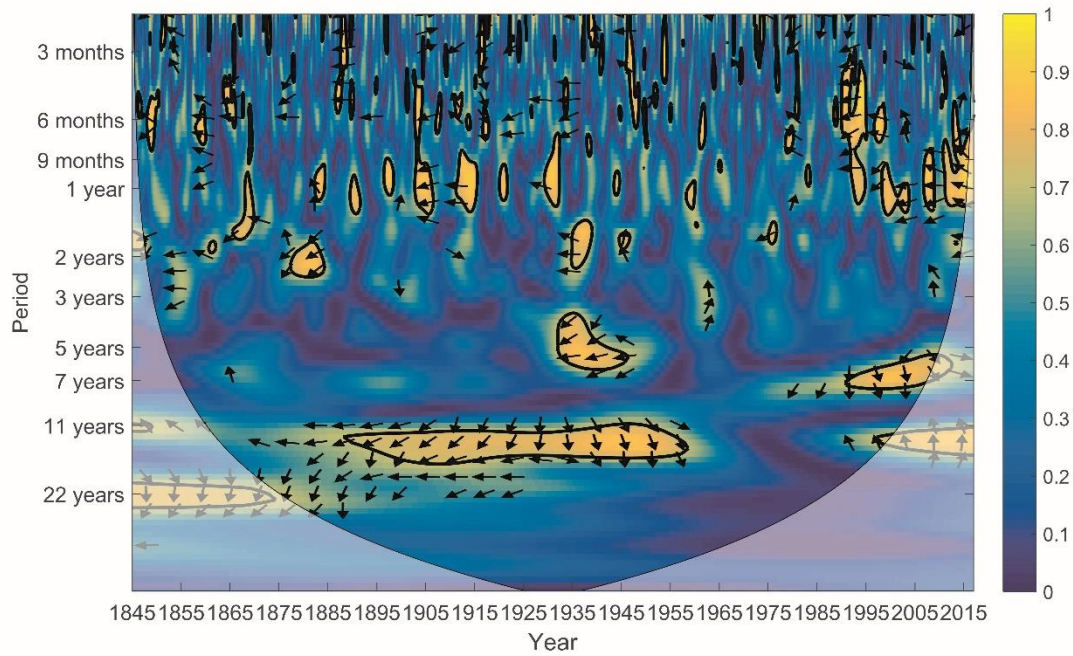
766 **Figure 12:** Time series, dimensionless wavelet spectrum (bottom right) and global wavelet
 767 spectrum (bottom left) of Lake Como monthly normalized inflow; 5% significance levels are
 768 marked with black contour lines in wavelet spectrum and COI; in global wavelet spectrum
 769 5% significance levels marked with the dashed red line.



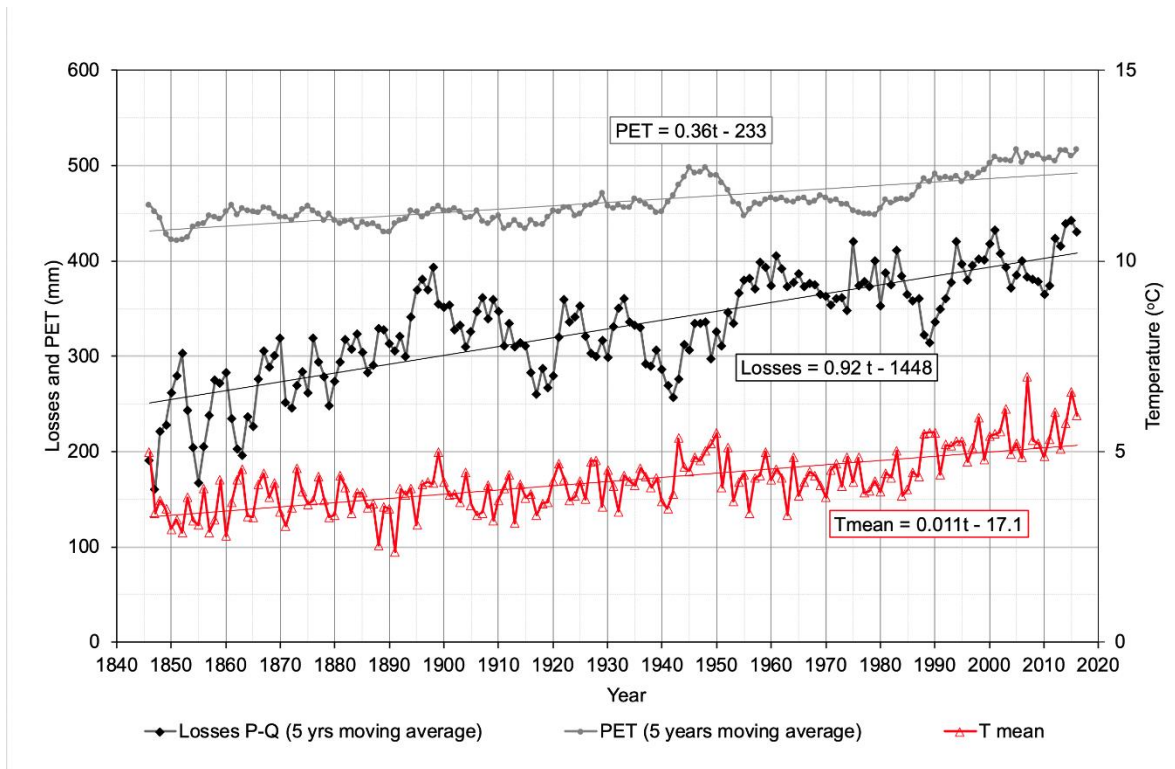
770 **Figure 13:** Linear regression trends of the wavelet energy spectrum of the inflows (a) and
 771 outflows (b) of Lake Como (Adda basin) for various characteristic scales.



772 **Figure 14:** Wavelet coherence spectrum of monthly sunspots and monthly precipitation, 5%
 773 significance levels marked with black contour lines and COI; arrows pointing to the right
 774 indicate in-phase between the two variables, arrows pointing down indicate that the first
 775 variable anticipates the second by $T/4$, with T being the wavelet scale, and left-pointing
 776 arrows indicate anti-phase.



777 **Figure 15:** Wavelet coherence spectrum of NAO monthly index and monthly precipitation,
 778 5% significance levels marked with black contour lines and COI; arrows pointing to the right
 779 indicate in-phase between the two variables, arrows pointing down indicate that the first
 780 variable anticipates the second by $T/4$, with T being the wavelet scale, and left-pointing
 781 arrows indicate anti-phase.



782

783 **Figure 16:** Annual losses, PET and mean temperature for the hydrological years 1846–2016.